Volume 16
Number 36
28 September 2024
Pages 6071–6292

Analytical Methods

rsc.li/methods

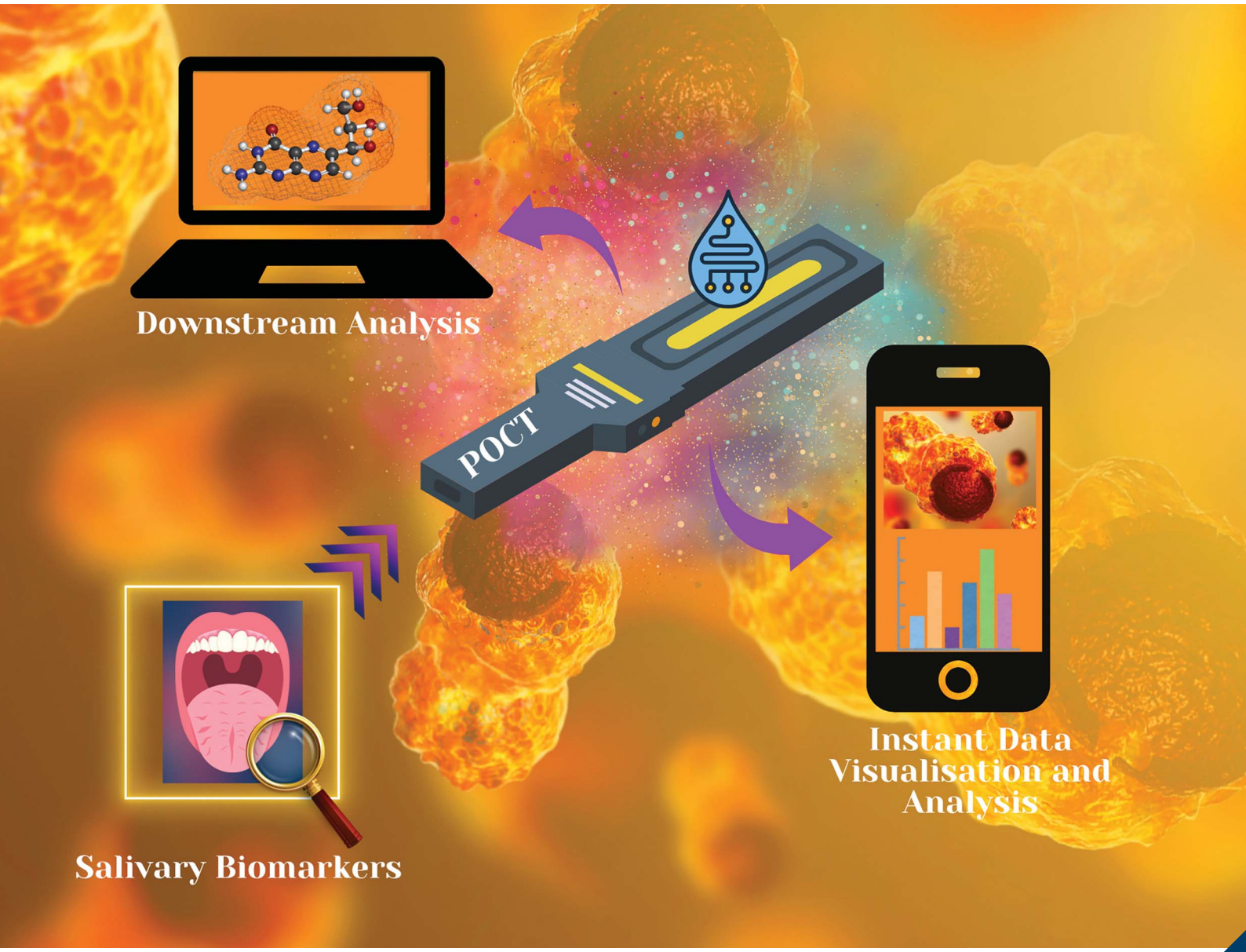

ISSN 1759-9679

ROYAL SOCIETY OF CHEMISTRY

CRITICAL REVIEW
Sanket Goel *et al.*
A review: early detection of oral cancer biomarkers using microfluidic colorimetric point-of-care devices

Indexed in Medline!

Analytical Methods

ROYAL SOCIETY OF CHEMISTRY

CRITICAL REVIEW

View Article Online
View Journal | View Issue

Cite this: *Anal. Methods*, 2024, **16**, 6098

A review: early detection of oral cancer biomarkers using microfluidic colorimetric point-of-care devices†

Aniket Balapure,[ab] Satish Kumar Dubey,[ac] Arshad Javed,[ac] Samit Chattopadhyay[d] and Sanket Goel *[ab]

Oral squamous cell carcinoma (OSCC) is the most common type of head and neck cancers. OSCC constitutes 90% of the head and neck malignancies. The delayed identification of oral cancer is the primary cause of ineffective medical treatment. To address this issue, low-cost, reliable point-of-care devices that can be utilized for large-scale screening, even in low-resource settings, including rural areas and primary healthcare centers, are of great interest. Herein, a comprehensive analysis of numerous salivary biomarkers that exhibit significant variations in concentration between individuals with oral cancer and those without is given. Furthermore, the article explores several point-of-care devices that exhibit potential in the realm of oral cancer detection. The biomarkers are discussed with a focus on their structural characteristics and role in oral cancer progression. The devices based on colorimetry and microfluidics are discussed in detail, considering their compliance with the 'REASSURED' criteria given by the World Health Organization (WHO) and suitability for mass screening in low-resource settings. Finally, the discourse revolves around the fundamental aspects pertaining to the advancement of multiplex, cost-effective point-of-care devices designed for widespread screening purposes.

Received 2nd June 2024
Accepted 2nd August 2024

DOI: 10.1039/d4ay01030b

rsc.li/methods

1. Introduction

TNM classification, devised by the Union for International Cancer Control, identifies oral cancer as a condition marked by the uncontrolled growth of malignant cells in different areas, including the lip as well as the oral cavity.[1] Oral squamous cell carcinoma (OSCC) represents a significant proportion of head and neck cancers, accounting for about 90% of such instances.[2] The high global prevalence of oral cancer has led to its designation as a major global health problem. Several strategies have been developed for the detection of different types of cancer.[3,4] Late detection of the disease is a significant contributing factor to the ineffectiveness of treatment strategies. Conventional diagnostic methods, including biopsy, cytopathology, and imaging adjuncts, are currently unable to detect the disease at its early stage.[5]

Visual examination of the patient cannot be used to identify disease stages I through IV. Thus, it is imperative to develop a screening system for accurate staging and early diagnosis that is ideal for mass screening in low-resource settings.[6] Liquid biopsies have garnered significant interest due to their potential for early diagnosis and the discomfort associated with the current tissue biopsy procedures.[7]

Oral cancer has been recognized as the sixth leading form of cancer worldwide, with India ranking second in the highest incidence of oral cancer cases. Fig. 1 depicts the spatial distribution of oral cancer throughout several regions of India.[8]

Thus, detecting oral cancer in the initial stage is of utmost importance to increase the individual's life expectancy. The predominant method employed for identifying oral cancer involves utilizing enzyme-linked immunosorbent assay (ELISA) to detect various biomarkers.[9,10] Various attempts have been made to develop ELISA.[11] However, it is constrained by the expensive cost of test kits and equipment and the long measurement times. Thus, there exists a necessity for affordable, easily operable, expeditious detection systems that are appropriate for large-scale screening and may be implemented in resource-constrained environments. Microfluidic devices are ideal for point-of-care applications owing to their low cost, simple operation, and suitability for limited resource settings.

[a]*MEMS, Microfluidics and Nanoelectronics (MMNE) Lab, Birla Institute of Technology and Science (BITS) Pilani, Hyderabad Campus, Jawahar Nagar, Kapra Mandal, Medchal District, 500 078, Telangana, India. E-mail: sgoel@hyderabad.bits-pilani.ac.in*

[b]*Department of Electrical and Electronics Engineering, Birla Institute of Technology and Science (BITS) Pilani, Hyderabad Campus, Jawahar Nagar, Kapra Mandal, Medchal District, 500 078, Telangana, India*

[c]*Department of Mechanical Engineering, Birla Institute of Technology and Science (BITS) Pilani, Hyderabad Campus, Jawahar Nagar, Kapra Mandal, Medchal District, 500 078, Telangana, India*

[d]*Department of Biological Sciences, Birla Institute of Technology and Science (BITS) Pilani, K K Birla Goa Campus, NH-17B, Zuarinagar, Goa 403726, India*

† Electronic supplementary information (ESI) available. See DOI: https://doi.org/10.1039/d4ay01030b

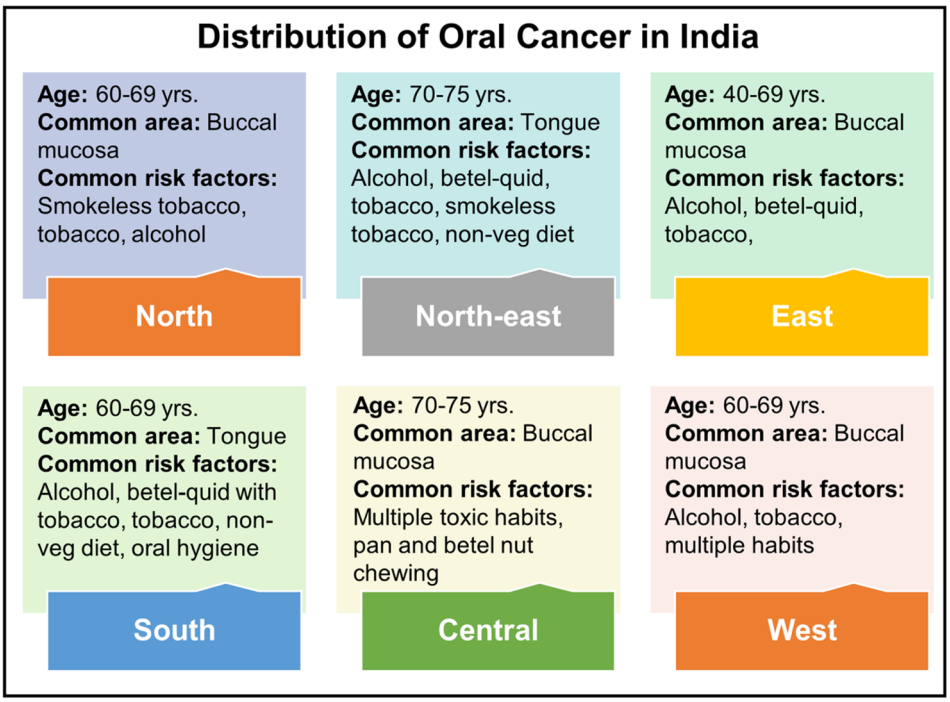

Fig. 1 The geographical distribution of oral cancer across India, with common affected areas and risk factors.[8]

'Microfluidics' refers to developing miniaturized devices and manipulating fluids within channels on the micrometer scale, with volumes ranging from 10^{-9} to 10^{-18} liters. Microfluidics technology was introduced in 1990, with the term "miniaturized total chemical analysis systems"—μTAS in the context that a single device can perform various laboratory steps.[12–14] Popular low-cost microfluidic devices include paper-based analytical devices (μPADs), digital microfluidics (DMF), lateral flow assays (LFAs), and wearable sensors. These are usually deployed for point-of-care testing (POCT) devices owing to their simplicity and rapid detection mechanism.[15–18] Microfluidics enables the detection of analytes from small volumes of the samples with great sensitivity, owing to the enhanced interaction kinetics between target molecules and surface biorecognition components facilitated by the high surface area to volume ratio. This facilitates a reduced assay time and lower cost in comparison to alternative protein quantification approaches.[19]

The study focuses on salivary biomarkers for detecting oral cancer, especially OSCC. It details the biomarkers' increased concentrations in oral cancer cases, their structure, and their role in detection and progression. Additionally, it examines low-cost microfluidic devices for oral cancer detection, with a significant focus on LFAs and paper-based colorimetric detection systems, highlighting their simplicity, affordability, and speed. In this study, the recently reported biomarker-based oral cancer detection was discussed in detail. The literature discussing biomarker concentration in clinical trials in oral cancer cases has been included, and an extensive list of the biomarkers is given along with several study details. Regarding the discussion on point-of-care devices, the literature discusses in detail several types of devices, such as colorimetric paper-based sensors, lateral flow assays (LFAs) with different detection systems, and gold and silver nanoparticle-based sensors, strictly adhering to REASSURED criteria and ideal for low resource settings have been included.

2. Samples for oral cancer detection

Invasive oral cancer detection and analysis samples include tumor tissue and peripheral blood cells.[20] Liquid biopsy is a commonly deployed technique for cancer detection. Various fluids, such as blood, pleural effusion, saliva, and urine, can be used to actively monitor oral cancer, including treatment response and patient conditions. In liquid biopsy, the detection objects are circulating tumor DNA, circulating tumor cells, and exosomes.[21] The mentioned samples are invasive, except for saliva and urine, and may distress patients. Non-invasive samples are vital for consistent patient biomarker monitoring.

Thus, sweat, saliva, tears, and urine are essential biological fluids for disease diagnostics and biomedical investigation. Among these biofluids, saliva is the most preferred sample owing to its accessible collection, transport, and low cost of storage. Moreover, saliva constitutes various hormonal, toxicological, immunological, and infectious disease biomarkers; thus, it has been used for oral health monitoring and cancer diagnosis.[22,23]

3. Oral cancer and related biomarkers

Treatment for advanced-stage disease frequently calls for complex multimodal treatment options linked to morbidity and subpar patient outcomes. OSCC has a high frequency of

advanced stage upon diagnosis and is asymptomatic in the early stages of the disease.[24] In recent times, surgical resection has been the primary way of OSCC treatment, depending upon the lesion's size. However, this procedure causes facial abnormalities and severe physiological dysfunction and impairs the food intake and linguistic capabilities of an individual.[25] The detection of biomarkers in various forms, including metabolites, miRNA, overexpressed proteins, *etc.* is the most efficacious approach for early diagnosis of OSCC.[26]

The structure, occurrence, and tandem of several reported oral cancer biomarkers are briefly discussed in the following section.

3.1. Reactive nitrogen species (RNS)

Some studies have demonstrated that premalignant lesion leukoplakia leads to the development of oral cancer through oxidative and nitrative stress. Reactive oxygen species (ROS) and other free radicals, after reacting with nitric oxide (NO) generate RNS. A transient species $NO^{\bullet}$ free radical, when generated at low concentration, plays a vital role in host defense and homeostasis. However, when generated in higher concentration and for a relatively longer time, it becomes mutagenic and genotoxic. $NO^{\bullet}$ may act as a mediator of DNA damage by producing RNS, inhibiting DNA damage-repair pathways, or forming carcinogenic nitrosamines. Salivary nitrates are important, which, upon conversion to nitrites (NO_2), induce carcinogenesis and act as a carcinogenesis promoter as they form carcinogenic nitrosamines, often reacting with amines and amides. Sometimes, these changes may occur because of old age due to a reduction in the protective salivary antioxidant mechanisms.[27]

3.2. Lactate dehydrogenase (LDH)

LDH is responsible for catalyzing the final step of the metabolic chain of anaerobic glycolysis and is present in almost all body cells. Oral cancer and several other potentially cancerous lesions and diseases have both been linked to elevated LDH levels.[28] Increasing LDH levels provide a highly acidic milieu that easily encourages metastasis and proliferation of tumor cells. Thus, elevated LDH levels are highly helpful in predicting metastasis of the neck lymph node. Moreover, Wanyong Jin *et al.* showed that an elevated LDH level can also be linked with the possibility of lymph node metastasis in the initial stages of OSCC.[29] Carcinogenesis has been observed to facilitate a shift in the energy transformation pathway, transitioning from oxidative phosphorylation to anaerobic glycolysis. The aforementioned phenomenon is frequently denoted as the Warburg effect. In this process, it is found that the LDH level increases and catalyzes pyruvate in lactic acid in the presence of electron donor NADH2. Thus, LDH is associated with the identification of malignant transformation. Another aspect that makes LDH a potential biomarker for oral cancer is that it can detect cellular damage or death, localization, and the surveillance of systemic changes and remains unaltered under normal conditions. Its presence in the saliva and serum makes it easily accessible for monitoring its levels.[30]

3.3. Cyclin D1(CycD1)

The 295 amino acid long CycD1 protein was initially discovered as the PRAD-1 putative oncogene. Multiple studies have shown a robust correlation between the activation of the CCND1 gene and/or the high expression of CycD1 and the occurrence of diverse malignant tumors. Furthermore, it has been discovered that the amplification of CCND1 has an impact on the regulation of CycD1, resulting in growth promotion, disruption, and carcinogenesis. The amplification of the CyclinD1 gene has been observed in around 22–58% of various human malignancies, and its prognostic usefulness in cancer patients is demonstrated by its clenched relationship to overall survival.[31] E2F1 and CycD1 are also involved in the cell cycle progression mediated by ribosomal protein L3 (uL3).[32] Moreover, several studies have confirmed the overexpression of CycD1 in oral cancer, and it is is a potential biomarker for early detection.[33]

3.4. Cytokines: IL-6 and IL-8

Cytokines are employed in the identification of cancer as well. T helper (Th) cells are known for their ability to produce interleukins and exert their effects on leukocytes. IL-6 is classified as a cytokine belonging to the interleukin family. It is important in several host-defense processes, encompassing hematopoiesis, immunological responses, and the activation of acute-phase reactions. Because of this, IL-6 is linked to the pathology of various cancers as well as immune-mediated inflammatory disorders (IMIDs).

Leukocyte activation and migration are predominantly mediated by chemokines, and are involved in a variety of immunological responses. A chemokine called IL-8 predominantly stimulates neutrophils for migration to the site of infection. The molecular weight of the glycosylated protein IL-6 is between 21 and 28 kDa. IL-6 comprises 212 amino acids with the four-helix bundle structure arranged in an up-up-down-down topology and an N-terminal signal peptide of 29 amino acids. IL-8 is a soluble, small peptide that has an 8–10 kDa molecular weight. IL-8 is an essential mediator in the regulation of inflammatory processes. Moreover, it also plays an essential role in triggering angiogenesis. The advancement and metastasis of cancer are particularly relevant to the pro-angiogenic characteristics of IL-8. On cancer cells, endothelial cells, tumor-associated macrophages, and infiltrating neutrophils, the IL-8 receptors are widely expressed. This proves that IL-8 has a substantial regulatory role in the tumor microenvironment. The development and viability of cancer cells are facilitated by IL-8 through autocrine signaling pathways.[34]

3.5. Cyfra 21-1

Cyfra 21-1 is also a well-known, recently studied biomarker for the detection of various cancers. The cleavage of the CK19 protein *in vitro* is mediated by the intrinsic caspase 3 activity, leading to the subsequent release of Cyfra 21-1 into the cancer cell lines. Furthermore, it is also reported that there is an elevation in the level of extracellular Cyfra 21-1 and a significant elevation in the levels of intracellular Cyfra 21-1 during

apoptosis. However, cell death due to caspase-independent death in the presence of the Z-VAD caspase inhibitor did not increase the Cyfra 21-1 level. Therefore, it has been postulated that the intracellular release of Cyfra 21-1 takes place during an intermediary phase of apoptosis triggered by caspase activation, subsequently leading to its release into the extracellular milieu.[35]

The concentration of Cyfra 21-1 can be detected from the serum or saliva. It is worth noting that the concentration of salivary Cyfra 21-1 was seen to be three times more than the concentration of serum Cyfra 21-1 in cases of oral squamous cell carcinoma (OSCC). Several other studies have also reported similar observations of higher salivary concentration of Cyfra 21-1 than that in blood serum in the case of OSCC. This makes Cyfra 21-1 a potential OSCC salivary biomarker. The importance of Cyfra 21-1 as a potential biomarker for OSCC was first revealed by Kurokawa *et al.* in 1997. Compared to controls and benign oral cancer patients, they found that patients with OSCC had a substantial rise in serum Cyfra 21-1. As per findings by Sugama *et al.*, increased serum Cyfra 21-1 results from cytokeratin release due to necrosis or cell lysis. Additionally, there is an increase in the cytokeratin breakdown due to epithelial transition to malignancy, resulting in a surge in the cytokeratin fragment concentration in the local environment.[36]

3.6. Tissue polypeptide antigen (TPA)

Another cytokeratin evaluated for oral cancer detection is tissue polypeptide antigen (TPA). A member of the intermediate filament family of proteins, cytokeratin is a helpful tool in the diagnosis of cancers. Upon an increase in the proteolytic activity in malignant cells, CK fragments are released into the bloodstream, and can be measured using specialized serological assays that are commercially available. Various studies have confirmed that, as opposed to healthy individuals, the CK level will be significantly high in patients with carcinoma.[37] It is a relatively older tumor maker in practice. It has been established that a combination of non-epidermal CK, such as CK8, 18, and 19, and TPA is immunologically linked. Through the S and G2 stages of the cell cycle, TPA is produced and released into the circulation throughout mitosis. Previous studies have provided evidence indicating that there is an elevation in the concentration of antigens in the sera and tumor tissues of individuals diagnosed with cancer, as opposed to the respective healthy controls. Nevertheless, owing to its wide-ranging specificity, the utilization of this particular marker as an indicator for tumors is infrequent.[38]

3.7. CA-125

CA-125 was discovered for the first time by American scientists in 1981. Known as Mucin 16 (MUC 16), the CA-125 glycoprotein is characterized by its high molecular weight, exceeding 200 kDa. It is known from the existing literature that it supports tumor growth by promoting metastatic invasion and suppression of natural killer cells. It is a long molecule consisting of three domains: the N-terminal, tandem repeat, and C-terminal. The tandem repeat domains and N-terminal are highly glycosylated and remain in the extracellular position. After proteolytic digestion, generally, the protein (extracellular portion) is released into body fluids.[39] Moreover, it is found that more than 80% of individuals with epithelial ovarian cancer have elevated serum CA-125 levels.[40]

3.8. CA 19-9

Cancer antigen 19-9 (CA 19-9), alternatively referred to as carbohydrate antigen 19-9, is a widely utilized and established biomarker for pancreatic cancer. It was first described by Koprowski *et al.* in 1979; later, in 1981, it was discovered that this molecule is present in the serum in the positive cases of colon and pancreatic cancer. It was also found that CA 19-9 is a constituent of glycoproteins and mucins. Mainly healthy human pancreatic and biliary ductal cells, as well as gastric, colon, endometrial, and salivary epithelia, generate CA 19-9. CA 19-9 exhibits overexpression in several inflammatory disorders, including pancreatitis and other benign gastrointestinal conditions.[41] Existing literature has established that CA 19-9 levels in the saliva of patients with OSCC were considerably altered compared to those in healthy individuals serving as controls.[42]

3.9. Carcinoembryonic antigen (CEA)

Carcinoembryonic antigen (CEA), one of the numerous tumor markers discussed, is a broad-spectrum serum cancer biomarker. CEA is a glycoprotein with a molecular weight of around 180 kDa. It serves as a significant cell-surface tumor marker and is present in several carcinomas. CEA is recognized as a prominent biomarker for gastrointestinal cancers, particularly in cases of colorectal malignancies.[43]

Numerous investigations revealed a favorable correlation between the occurrence, progression, and severity of oral cancer and the concentration of CEA in serum. However, the existing diagnostic aids are not sufficient for accurate and sensitive detection, leading to proper, early stage oral cancer prediction. Numerous interfering components in the blood hindered the accurate and precise detection of CEA. Therefore, compared to blood, saliva is an effective tool for CEA concentration monitoring, as it consists of minimal interfering substances, and the sample collection is painless and non-invasive, which is highly useful in point-of-care testing. The average concentration in healthy individuals remains 0.1–2.5 ng mL^{-1}, which eventually increases to nearly 5 ng mL^{-1} in the case of early stage tumor development.[44]

3.10. Squamous cell carcinoma antigen (SCCA)

Squamous cell carcinoma antigen (SCCA) was first introduced by Kato and Torigoe in 1977 and found to be useful as a tumor-specific antigen for the detection of squamous cell carcinoma in the uterine cervix. However, it was found that its diagnosis efficiency for OSCC was unsatisfactory.[45] SCCA has two highly homologous isoforms, SCCA1 and SCCA2, encoded by *SERPINB3* and *SERPINB4* genes, respectively, and is located on the long arm of chromosome 18 (18q21.3). The proteins SCCA1 and SCCA2, alternatively known as SERPINB3 and SERPINB4, are members of the serine protease inhibitor family (SERPINBs). They are characterized by an ovalbumin-like domain containing nine α-helices and three antiparallel β-sheets. Additionally,

these proteins possess a reactive center loop that plays a crucial role in their ability to bind to and inhibit the target protease.[46]

SCCA is a 48 kDa protein that is also used for the detection of lung cancer. SCCA has also been explored for the diagnosis of OSCC, and efforts have been made to improve the detection efficiency for the diagnosis of OSCC. M. Yang *et al.* developed a straightforward, efficient, and scalable approach utilizing saponin treatment for the identification of intra-vesicular proteins of extracellular vesicles (EVs) without the need for additional purification procedures. This strategy works by elevating the SCCA concentration in the serum, thus resulting in improved diagnostic efficiencies of SCCA for OSCC.[47]

3.11. Kiel 67 (Ki-67)

The Ki-67 antibody is generally used to localize the Ki-67 protein in the tissue sections. The Ki-67 antibody was named after its characterization in Kiel, Germany. Additionally, it is worth noting that the antibody was cultivated in the 67th well of the tissue culture plate. The Ki-67 protein is located in the nucleus as detected by immunolocalization of the Ki-67 antigen, and its gene is located on chromosome 10q25-ter.[48] The Ki-67 proliferation rate is an additional biological and predictive indicator. The expression of Ki-67 antigens is initiated during the S-phase and progressively increases during the S and G_2 phases, ultimately peaking during mitosis. Following cell division, the cells enter the G_1 phase, wherein they possess a supply of Ki-67 antigen. Throughout this phase, the level of Ki-67 antigen gradually diminishes, resulting in an extended G_1 phase. Throughout the cell cycle, the Ki-67 protein is expressed in proliferating cells but not in quiescent (G_0) cells.[49] Multiple studies have provided evidence of the considerable prognostic importance of enhanced proliferative activity in certain forms of cancer. The Ki-67 protein is widely recognized as a proliferation marker, serving as an indicator of the overall proportion of proliferating cells in a tumor.[50]

3.12. Insulin-like growth factor-I (IGF-I)

Investigations have provided evidence suggesting that the IGF type I receptor (IGF-IR) and its ligands IGF-I and IGF-II have a role in the development and progression of many cancers in humans.[51] The receptor tyrosine kinase family includes the insulin-like growth factor-I (IGF-I) receptor (IGF-IR). The molecular configuration comprises two α- and two β-subunits that are interconnected through disulfide bonds. The α-subunits are situated extracellularly and play a role in binding ligands, but the β-subunits span the plasma membrane and possess an intracellular kinase domain that is specifically responsible for initiating signal transduction cascades.[52] One of the plausible reasons that IGF-I is associated with various types of cancers is its role in angiogenesis, apoptosis, differentiation, proliferation, and metabolism.[53]

3.13. Metalloproteinases MMP-2

Matrix metalloproteinases (MMPs) represent a group of proteinases that rely on zinc for their enzymatic activity. These proteinases are first secreted in an inactive form, known as proenzymes, and necessitate proteolytic cleavage to attain their active state. The association between MMP-2 and MMP-9 and the malignant traits of tumor cells has been well established. Nevertheless, a notable disparity was noted in the activation of MMP-2 compared to MMP-9 in malignant OSCC. An increased activation ratio of MMP-2 exhibits a substantial correlation with lymph node metastasis in OSCC and can serve as a potential predictor of the risk of metastasis development. Therefore, MMP-2 possesses the potential to serve as a more specific molecular target for anti-metastatic therapy for OSCC.[54] It is also known from the literature that MMP-2 and MMP-9 play a significant role in type IV collagen degradation, a significant component of the basement membrane, which is a prerequisite for tumor invasion.[55] Thus, based on the substantial research

Table 1 List of salivary biomarkers and the percentage change observed in the OSCC in several clinical studies

Classification of chemicals	Salivary biomarker	% change observed	Related disease	Clinical/preclinical study	References
Carbonyl compounds	Carbonyls	246	Tongue cancer	Clinical	56
Proteins	Kiel 67 (Ki-67)	127		Clinical	
	Lactate dehydrogenase (LDH)	86	Oral cancer and oral submucous fibrosis	Clinical	
	Cyclin D1(CycD1)	87	Tongue cancer	Clinical	
	Interleukin 6 (IL-6)	6200	OSCC	Clinical	59
	Interleukin 8 (IL-8)	200		Clinical	
	Cyfra 21-1	400		Clinical	69
	CA125			Clinical	
	Tissue polypeptide antigen			Clinical	
	CA 19-9	~300		Clinical	
	CEA	~170		Clinical	
	Squamous cell carcinoma antigen (SCCA)	~170		Clinical	
	Insulin-like growth factor-I (IGF-I)	117		Clinical	70
	Metalloproteinases MMP-2	75		Clinical	
Reactive nitrogen species (RNS)	NO	60		Clinical	71
	NO_2	190			
	NO_3	93			

Table 2 A list of recently reported salivary biomarkers obtained from the clinical studies has been provided. The table also gives the detection method, sample size, and final outcomes of the study

Year	Salivary biomarkers	Type of cancer	Detection method	Number of samples/ patients under investigation	Outcomes	References
2024	miRNAs (miR-7-5p, miR-10b-5p, miR-182-5p, miR-215-5p, miR-431-5p, miR-486-3p, miR-3614-5p, and miR-4707-3p)	Oral cancer	Quantitative real-time polymerase chain reaction (PCR)	Oral cancer, $n = 50$; oral potentially malignant disorders, $n = 52$; controls, $n = 60$	Salivary miRNA can be deployed in diagnosing and predicting oral cancer	72
2024	Methylation statuses of genes TRH, RASSF1A, p16, and MGMT	Oral tongue squamous cell carcinoma (OTSCC)	mRNA sequencing	OTSCC patients = 45 and healthy control = 20	Salivary DNA methylation as a predictive OTSCC biomarker	73
2024	Matrix metalloproteinase-1 (MMP-1)	OSCC	Time-saving rapid strip test (RST) for MMP-1	$n = 196$ OSCC patients, $n = 236$ patients with oral potentially malignant disorders, and $n = 171$ healthy controls	Salivary MMP-1 can be deployed for the detection and monitoring of OSCC	74
2024	Human beta-defensin 3 (hBD-3)/human beta-defensin 2 (hBD-2)	OSCC	96-Well immune-plates	$n = 40$ subjects; $n = 54$ for the tissue immunofluorescence microscopy study	The beta-defensin index can be a functional biomarker for oral cancer detection	75
2024	Cellular prion protein (PrP^C)	OSCC	Enzyme-linked immunosorbent assay (ELISA)	$n = 76$ OSCC patients, $n = 30$ oral potentially malignant disorders (OPMDs) patients, and $n = 78$ control	PrP^C in saliva and serum can be a potential biomarker for early diagnosis of OSCC	76
2024	Alpha-2HS-glycoprotein (AHSG)	Oropharyngeal cancer (OPC)	High-throughput proteomics technique, tandem Mass Tag (TMT) based quantification of salivary proteins	Discovery phase: 20 OPC cases Validation phase: 41OPC cases	AHSG levels are elevated in the saliva of OPC patients as opposed to healthy controls	77
2023	MALAT1	OSCC	Quantitative real-time polymerase chain reaction (PCR) and histopathological examination	$n = 20$ OSCC patients and $n = 20$ healthy controls	Higher expression of MALAT1 and lower expression of miRNA-124 in OSCC	78
2022	miRNA-1307-5p	OSCC	Flow cytometry	$n = 12$ saliva samples	Exclusively overexpressed in tissues and salivary exosomes in OSCC	79
2022	Exosomal MicroRNA-486-5p and MicroRNA-10b-5p	Oral and oropharyngeal squamous cell carcinoma	Quantitative real-time PCR	$n = 50$	miR-486-5p: elevated and miR-10b-5p: reduced in oral and oropharyngeal squamous cell carcinoma	80
2020	Exosomal miR-24-3p	OSCC	miRNA microarray analysis and qRT-PCR	$n = 45$ OSCC patients and $n = 10$ normal controls	miR-24-3p expressed at a higher level in OSCC	81

Table 2 (*Contd.*)

Year	Salivary biomarkers	Type of cancer	Detection method	Number of samples/ patients under investigation	Outcomes	References
2020	Lactate dehydrogenase (LDH), C-reactive protein (CRP), and cancer antigen 125 (CA125)	Oral lichen planus (OLP) and OSCC	Enzyme-linked immunosorbent assay (ELISA)	$n = 15$ OSCC patients, $n = 20$ OLP patients, and $n = 20$ healthy controls	Salivary LDH, CA125, and CRP can be deployed to evaluate malignant changes	82
2020	Matrix metalloproteinase-1 (MMP-1)	OSCC	Developed ELISA	$n = 269$ OSCC patients, $n = 578$ oral potentially malignant disorder (OPMD) patients, and $n = 313$ healthy controls	Developed MMP-1 ELISA can be deployed for OSCC identification and monitoring	83
2019	Tropomyosin alpha-4 chain (TPM4)	OSCC	Two-dimensional polyacrylamide gel electrophoresis and mass spectrometry	$n = 30$ OSCC patients and $n = 30$ healthy controls	Salivary upregulation of TPM4 in the case of OSCC	84
2017	miR-486-5p and miR-10b-5p	Head and neck squamous cell carcinoma (HNSCC)	Droplet digital PCR	miRNA-seq pilot: $n = 5$ and $n = 5$ healthy controls ddPCR assays: $n = 11$ and $n = 9$ healthy controls	miR-486-5p: Upregulated miR-10b-5p: downregulated	85
2016	C-Reactive protein (CRP)	Oral premalignant lesions and OSCC	Immunoturbidimetry method	$n = 20$ OSCC patients, $n = 20$ oral premalignant patients, and $n = 20$ healthy controls	Higher CRP levels in OSCC and oral premalignant lesion cases	86
2011	γ-Aminobutyric acid, phenylalanine, valine, *n*-eicosanoic acid and lactic acid	OSCC	Ultra performance liquid chromatography coupled with quadrupole/time-of-flight mass spectrometry and multivariate statistical analysis	$n = 37$ OSCC patients, $n = 32$ oral leukoplakia (OLK) patients, and $n = 34$ healthy subjects	Oral cancer can be detected using salivary metabolome diagnostics	87

conducted so far, it can be inferred that MMP-2 is a noteworthy biomarker for detecting oral cancer.

3.14. Carbonyls

Carbonyls are the products of protein oxidation. The substantial increase in the salivary carbonyls can be attributed to the exposure of the epithelial cells to the substantial free radical attack. Moreover, in the malignant tissues, the extent of oxidative DNA damage was also attributed to the reduction in the total antioxidant capacity, resulting in an increase in free radical concentration.[56] Thus, carbonyls are also a potential biomarker for OSCC diagnosis and monitoring.

Various reviews are dedicated to oral cancer biomarkers; the reader is advised to go through them for a thorough understanding. Moreover, there are several recently published review articles discussing the salivary biomarkers for the detection and monitoring of OSCC and other oral cancers, and readers are advised to go through an extensive list of the salivary biomarkers.[57–68] Several salivary biomarkers that exhibit notable variations in concentration in cases of OSCC patients in clinical studies and other types of oral malignancies are given in Table 1. The biomarkers discussed in Table 1 are ideal for the development of point-of-care devices owing to the significant increase in concentration observed in the case of oral cancer. Apart from the discussed biomarkers, there are several other recently explored salivary biomarkers that are also linked to the detection and progression of oral cancer and tested using clinical samples, which are listed in Table 2.

4. Salivary metabolites for oral cancer detection

As we have discussed so far, various salivary biomarkers are known to change significantly in oral cancer compared to healthy controls. Metabolites are the small molecules involved in metabolic reactions.[88–90] Various metabolites are released into the saliva by blood.[91] As a result, salivary metabolites are also an important class of small molecules that can be deployed for early oral cancer detection and can be considered powerful early screening tools.[92–97] Herein, we have given a list of selected metabolites that are known to change concentration significantly in the case of OSCC. Metabolites such as 3-phenylpropionate, cytosine, hexanoate, 3-(4-hydroxyphenyl)propionate, and *S*-adenosylmethionine are found to increase by 627%, 604%, 467%, 395%, and 348% respectively. Various additional metabolites exhibit a substantial increase in concentration, which depends upon the timing of saliva collection. The extensive list and the change in the absolute concentration values can be found in the review by Shigeo Ishikawa *et al.*[98] There are several other studies that have listed and discussed salivary metabolites in detail.[95,99]

5. The cancer treatment and the concentration of biomarkers

The detailed discussion of cancer metabolism and its significance in clinical application can be seen in the review by Honigova *et al.*[100,101] The stage of the disease determines how oral cancer, or any other cancer in general, will be treated. Surgery can be used to treat early stage identification, but a multidisciplinary approach is needed for advanced-stage identification.[102] In the case of OSCC, it is mainly managed with surgery; however, radiotherapy and chemoradiotherapy are used post-operatively for disease control.[103] Immune checkpoint blockade (ICB) therapy has been used for OSCC since 2016 and has been found to have a low response rate and adverse events.[104]

It has been found that little attention has been given to monitoring the levels of different salivary biomarkers and metabolites throughout and after treatment, such as chemotherapy, radiation, and immunotherapy. A detailed cohort study is required for various biomarkers and their concentration during the disease and treatment progression.

6. 'ELISA': a conventional gold standard method for oral cancer detection

The application of immunoassays for the identification of infectious disorders can be traced back to the year 1917 when they were initially employed for the rapid identification of antigens through interaction with antibodies. Enzyme-linked immunosorbent assay (ELISA) and radioimmunoassays (RIA) represent two prominent immunoassay-based platforms that have undergone substantial investigation to develop novel, highly sensitive, and point-of-care diagnostic tools for disease detection. Currently, ELISA continues to be widely utilized as a prevalent immunoassay technique for identifying and quantifying biomarkers within laboratory settings.[105–108] ELISA techniques rely on the selective binding interactions between antigens and antibodies for target proteins in body fluids. Nevertheless, the limited sensitivity of these methods restricts their utilization in modern laboratory protocols.[109]

Moreover, the utilization of ELISA is again constrained by the expensive test kits, equipment, long measurement time, and the challenges encountered when attempting multiplexing. Therefore, ELISA is not typically the preferred option for the implementation of point-of-care diagnostics.[110]

The search for innovative, cost-effective, and user-friendly point-of-care devices designed for the diagnosis of oral cancer in low-resource settings concludes with microfluidic devices which are discussed in detail in the following sections.

7. Microfluidic devices

Recently, research interest has grown in 'micro total analysis systems' (μ-TASs) or 'lab-on-chip' (LOC). There are generally two main approaches in microfluidics. The first is combining microsensors with fluidic components such as a pump and flow chips, and the other is miniaturizing various analytical chemical methods.[111] Moreover, extensive research is focused on the 'organ-on-a-chip' (OoC) for pre-clinical and clinical translational precision. The current research is centered around

streamlining the intricate nature of human organ architecture, specifically elucidating its fundamental cellular microanatomy. This simplification enables a detailed investigation into the mechanisms underlying drug action, absorption, metabolism, and other related processes.[112–118]

Another fascinating approach used in microfluidic systems is 'origami,' which is the folding of paper. Origami is used in various applications such as tissue engineering, tissue scaffolds, drug delivery, stents, catheters, *etc.*[119] Another low-cost and effective microfluidic device for point-of-care (POC) testing is lateral flow assays (LFAs), also known as lateral flow test strips (LFTSs). Cellulosic paper and plastic supports are the first choices to maintain the low cost of the fabrication of LFAs. In addition to the low cost, the World Health Organization (WHO) insists that all the POC devices must follow the REASSURED criteria, *i.e.*, real-time connectivity, ease of specimen collection, affordable, sensitive, specific, user-friendly, rapid and robust, equipment-free, and delivered to the end-users. Numerous LFAs reported to date for various cancer-related biomarkers can be seen in the review by Mahmoudi *et al.*[120–122]

7.1. Colorimetric paper-based sensors

Colorimetric sensors rely on the alteration in color when the analyte of interest is present, as implied by their name. The colorimetric signal can be detected with the naked eye. Paper-based sensors are successfully deployed for qualitative and semiquantitative measurements. Colorimetric paper-based analytical devices (PADs) include spot tests, LFAs, dipsticks, and 2D/3D μPADs. Dipsticks are not so popular for cancer detection owing to their requirement of high volume of samples.[123]

7.1.1. Lateral flow assays (LFAs). LFAs have gained recognition as prominent POC devices due to their efficacy in qualitative, semi-quantitative, or quantitative detection of several biomarkers.[124–127] LFAs working with various detection systems can be categorized as colorimetric, luminescent, magnetic, electrochemical, surface-enhanced Raman spectroscopy (SERS), and thermal detection, as shown in Fig. 2.[128] It is essential for the detection system to have powerful signal amplification for the precise detection of various analytes. Herein, various LFAs with different detection systems are discussed in detail. Fig. 2 shows various detection systems deployed in the LFAs.

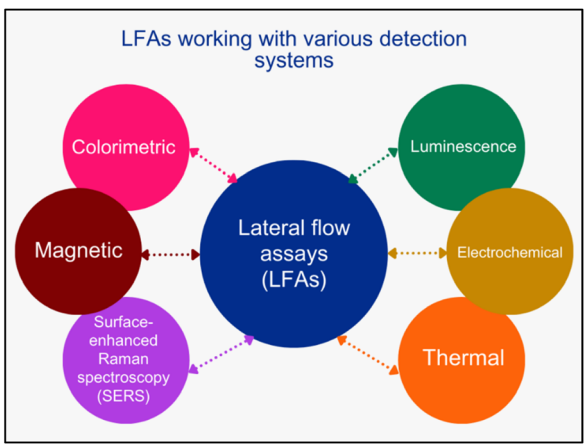

Fig. 2 Schematic showing various detection systems used in LFAs.

7.1.2. Basic working principle of LFAs. The critical component of the LFA is a nitrocellulose (NC) membrane, which provides the platform for the reactions during the analysis. The antibodies interact with the nitrate ester through the peptide bond and strong dipoles of the ester, resulting in the electrostatic interaction. After the interaction of the antibodies on the test membrane, it is dried so that the antibodies remain fixed on the test NC. Polyvinyl alcohol is used to inhibit the activity of free active sites on the membrane. The sucrose solution forms a hydrated glaze that is quickly and efficiently dissolved when the aqueous sample is dropped and helps in the unrestricted mobility of the labeled antibodies. In this way, a test region and a control region are developed. The bio-recognition elements, *i.e.*, captured molecules, remain on the NC in the respective test or control region *via* hydrogen bonds, electrostatic interaction, and/or hydrophobic forces. Capillary forces drive the sample movements on the NC; the specific interaction, depending on the sample type, occurs in the test region (T-line) and the control region (C-line), giving the results of the conducted test depending on the types of the antigen to be detected and the antibodies deployed. Depending on the type of detection mechanisms deployed, it can be divided into sandwich format and competitive format LFAs. Details of this can be seen in the review by Elif Burcu Bahadır *et al.*[129] The basic working principle of an antibody-antigen-antibody sandwich LFA is shown in the following schematic, in Fig. 3.

Here, selected recently reported LFAs, which are based on various detection mechanisms, are discussed. Several detection systems, including distance-based, lanthanide-based, cascade nucleic acid amplification, upconversion nanoparticle, and immuno-sandwich assay, are discussed in detail.

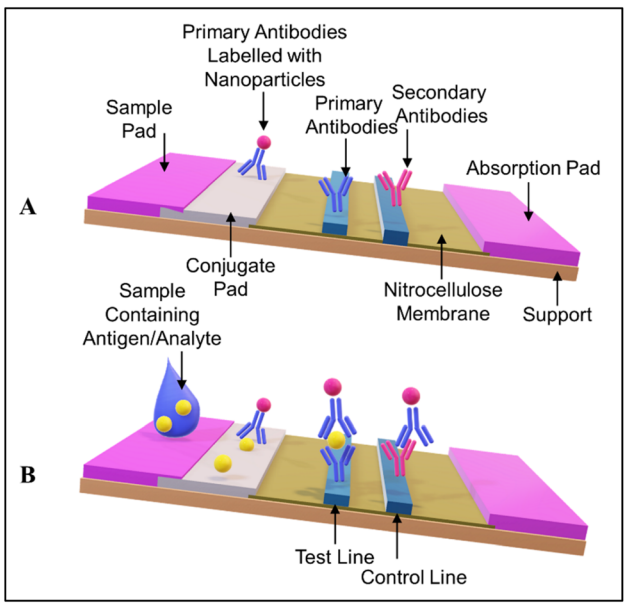

Fig. 3 (A) The architecture of a standard LFA. (B) Basic working principle of an antibody-antigen-antibody sandwich LFA.

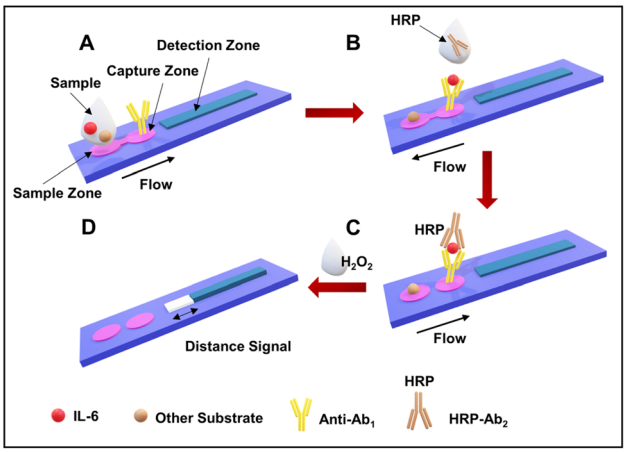

Fig. 4 Assay workflow of B-dPADs for IL-6 detection. (A) Sample addition and the binding of antibodies. (B) The addition of the secondary HRP-labeled antibodies. (C) The flow of liquid in the capture zone and then in the detection channel. (D) The quantification of the bleaching observed in the detection channel. Reproduced/re-drawn with permission from ref. 130. Copyright 2022 American Chemical Society.

7.1.3. Distanced-based colorimetric detection. Recently, a distance-based paper sensor (dPADs) was developed by Kawin Khachornsakkul *et al.* The paper-based analytical device could quantitatively detect interleukin-6 (IL-6) from human saliva and urine samples. They proposed a hydrophilic bridge valve coupled with a dPAD (B-dPAD) for distance-based colorimetric immunoassay. This approach helps in the reduction of washing steps, the time required, and the complexity involved, and it improves the analytical performance. The measuring step entails methylene blue (MB) decomposition utilizing hydrogen peroxide (H_2O_2). The developed B-dPADs comprise three distinct regions: a sample zone, a capture zone, and a detection zone. Two hydrophilic bridge valves separate these regions. The workflow is shown in Fig. 4.

The fabricated B-dPADs were evaluated for IL-6 quantification in the range of 0.05–25.0 pg mL^{-1} (see Fig. 5). The measurement of the detection zone was conducted using a conventional ruler and subsequently graphed. The bleaching length was linear in the tested range and was suitable for the clinical range of 5.0–15.0 pg mL^{-1}, with an R^2 value of 0.9992.[130]

7.1.4. A lanthanide-based fluorescence detection system. Lanthanide-based LFAs are extensively employed techniques, with particular emphasis on the utilization of Eu(III) chelates. These chelates exhibit notable and appealing properties, including time-resolved fluorescence and a significant Stokes shift. A novel mini-emulsion polymerization technique was employed by Zhenhua Li *et al.* to produce carboxyl-modified fluorescent microspheres (referred to as OS-EuCM) achieved through a one-step process. The OS-EuCM microspheres exhibited favorable attributes such as high stability, specific adhesion, and uniform distribution of particle sizes. These characteristics were superior to those of conventional microspheres obtained using the swelling method.

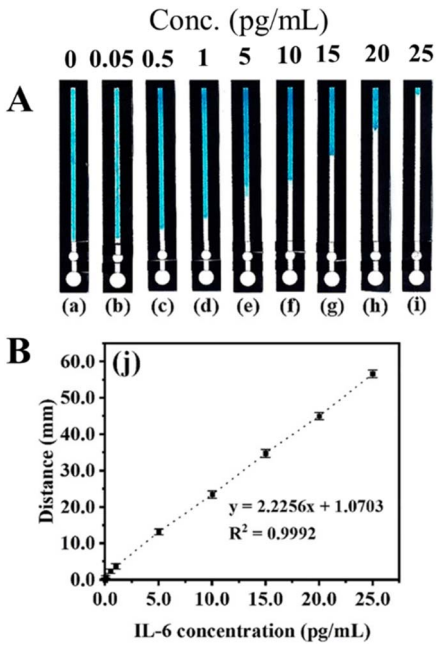

Fig. 5 (A) Photographs of devices with the IL-6 assay performed at various concentrations. (B) The calibration curve. Reproduced with permission from ref. 130. Copyright 2022 American Chemical Society.

The developed LFAs were used for the detection of alpha-fetoprotein, a tumor marker. The increased sensitivity and specificity exhibited by the developed LFA make it highly suitable for diagnostics in clinical settings. LFAs could detect a higher concentration of 320 ng mL^{-1}, with a detection limit of 0.683 ng mL^{-1}. A schematic representation of the structure of the OS-EuCM, biconjugation process, and fabrication of the LFA is shown in Fig. 6.

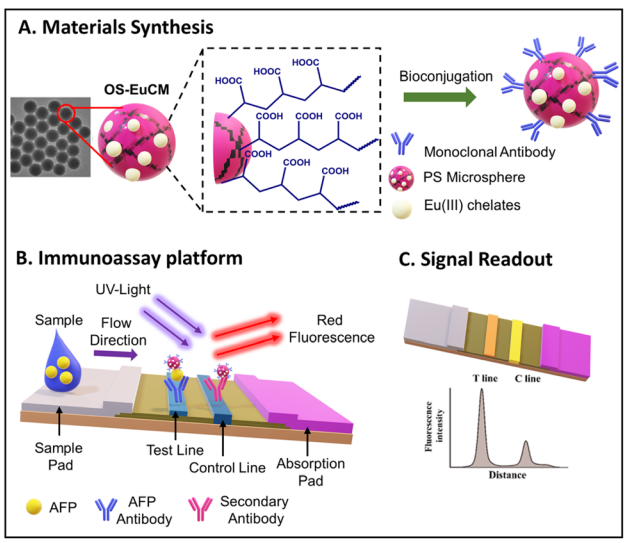

Fig. 6 A schematic representation of the structure and bioconjugation process of OS-EuCM, as well as the corresponding fabrication of lateral flow immunoassays (LFIAs) for detecting AFP. Reproduced/re-drawn with permission from ref. 131. Copyright 2021 Chinese Society of Rare Earths.

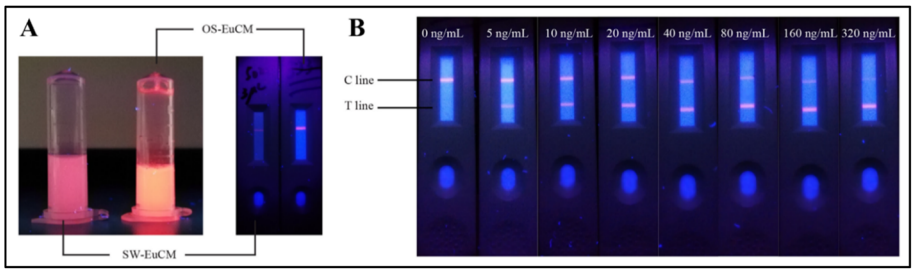

Fig. 7 (A) The photographs depict two distinct types of microsphere solutions and strips after film drawing, each containing identical solid contents, which were subjected to irradiation at a wavelength of 365 nm. (B) Optical images of tested strips exhibiting various alpha-fetoprotein (AFP) concentrations under irradiation at a wavelength of 365 nm. Reproduced with permission from ref. 131. Copyright 2021 Chinese Society of Rare Earths.

OS-EuCM shows better fluorescence intensity under ultraviolet (UV) light as opposed to conventional microspheres synthesized using the swelling method shown in Fig. 7(A). OS-EuCM was used for the fabrication of test strips, as shown in Fig. 7. Succinctly, following the pre-mixing of the serum sample with the OS-EuCM labeled AFP-specific antibody, the resulting complexes were introduced onto the sample pad and subsequently passed over the nitrocellulose membrane. The concentration of AFP in the sample exhibited a direct relationship with the ratio of H_T/H_C. H_T and H_C are the fluorescence peak heights for the test and control lines, respectively. The various concentrations tested and the optical images of the strips are shown in Fig. 7(B).[131]

The fabricated strips were tested for AFP concentration in the range of 0–320 ng mL^{-1} under irradiation at a wavelength of 365 nm, as shown in Fig. 7(B).

7.1.5. Cascade nucleic acid amplification (HRCA)-based colorimetric detection. Another LFA with the HRCA mechanism was developed and deployed for the detection of miRNA 31 for OSCC diagnosis by Wenna Li *et al.* The miRNA under investigation demonstrated complementary sequences with both biotin-modified probes (referred to as b-Lcp) that were affixed to Streptavidin-modified magnetic beads, as well as with initiator strand probes (referred to as Dp). With target miRNA, it initiates hybridization with b-Lcp and Dp, resulting in the formation of the sandwich structure.

They have employed two specific probes acting as the primer for the rolling circle amplification (RCA) reaction. After various series of subsequent reactions, the final blue color signal was observed on the streptavidin-labeled strip.

The detailed schematic of the working principle is given in the following Fig. 8.[132]

7.1.6. Upconversion nanoparticle-based luminescence detection system. Upconversion nanoparticles (UCNPs) belong to a distinctive category of optical nanomaterials and are usually obtained by lanthanide ion doping. These nanoparticles exhibit a wide range of electronic transitions within their 4f electron shells and can undergo up-conversion, a process when two or more photons with lower energy levels are converted into a single photon with higher energy levels.[133] Wanghong He *et al.* developed an LFA by deploying core–shell upconversion nanoparticles (G-UCNPs) as a luminescent probe. The developed

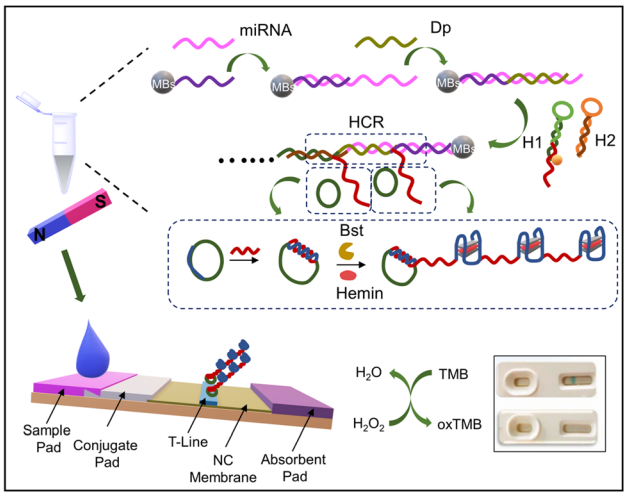

Fig. 8 LFA: based on the cascade nucleic acid amplification technology for miRNA 31 for OSCC diagnosis. Reproduced/re-drawn with permission from ref. 132. Copyright 2022 Elsevier B.V.

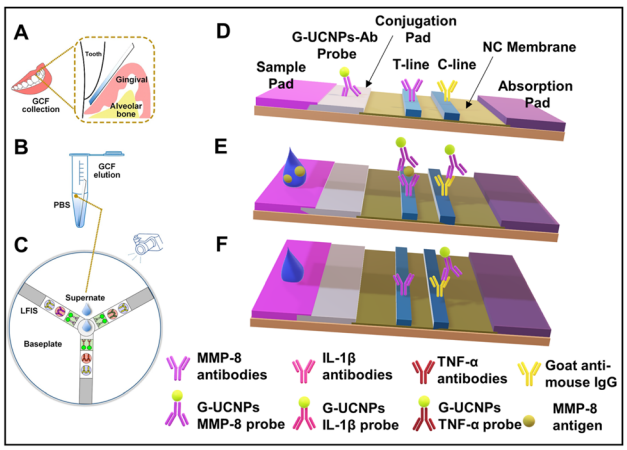

Fig. 9 Working principle of the developed upconversion nanoparticle based LFA. (A) Sample collection, (B) sample elution, (C) disk-like detection platform, and (D–F) schematic showing the working principle. Reproduced/re-drawn with permission from ref. 134. Copyright 2021 Elsevier B.V.

Table 3 A summary of recently reported LFAs with colorimetric and fluorescence-based detection systems

Biomarker/ bioanalyte	Detection mechanism	Tag/signal amplification	Type of sample	Sample volume	Detection time	Linear range	LOD	Ref.
Helicobacter pylori	Fluorescence	Time-resolved fluorescent microspheres	Saliva	60 μL	8 min	101–105 CFU mL^{-1}	102 CFU mL^{-1}	135
Human osteopontin (OPN) protein	Colorimetric	Streptavidin-modified gold nanoparticles	Serum	20 μL	5 min	10–500 ng mL^{-1}	0.1 ng mL^{-1}	136
Human epidermal growth factor receptor 2 (HER2)	Colorimetric	Biotin-modified aptamer modified gold nanoparticles	Serum	Not given	30 min	0–99 nM	24 nM	137
Prostate-specific antigen	Colorimetric	Platinum nanoparticles	Serum	Not given	30 min	0–12 ng mL^{-1}	0.54 ng mL^{-1}	138
Alpha-fetoprotein	Fluorescence	Lanthanide-based carboxyl-modified fluorescent microspheres	NA	110 μL	Not given	0–320 ng mL^{-1}	0.683 ng mL^{-1}	131
Human papillomavirus (HPV) type 16 DNA	Colorimetric	Copper oxide nanoparticles	NA	30 μL	20 min	5–100 nM	1.0 nM	139
Helicobacter pylori with cytotoxin-associated protein (CagA)	Fluorescence	CdS quantum dots	Serum	Not given	Not given	Not given	20 pg mL^{-1}	140
Human papilloma virus (HPV): HPV16 and HPV18	Colorimetric	Gold nanoparticles and CIALFB (CRISPR/Cas-isothermal amplification based LFB)	Cervical exfoliated cell samples	2–4 μL	<60 min	Not given	3.1 attomoles (∼1.8 copies)	141
β-Galactosidase	Colorimetric and fluorescence	The recombinant spores and gold nanoparticles	NA	100 μL	15–20 min	Not given	10^{-15} mol	142

multiplex LFA was used for the detection of three periodontitis biomarkers in gingival crevicular fluid (GCF), matrix metalloproteinases-8 (MMP-8), interleukin-1 beta (IL-1β) and tumor necrosis factor-alpha (TNF-α).

The working principle is shown in Fig. 9. A sterile Whatman strip was used for GCF sample collection, and the strip was transferred to a sterile Eppendorf tube and eluted (as shown in Fig. 9(A) and (B)). The amount of the sample was also taken into consideration for accurate measurements. The sample was introduced to a disk-like platform, where there will be an interaction with the three kinds of pre-added probes for the detection of MMP-8, IL-1β, and TNF-α, T, and C lines (Fig. 9(C)). The immune-sandwich assay was the basis of the detection mechanism. The general detection mechanism can be discussed by using the example of MMP-8. MMP-8 antigens from the samples bind specifically with detection antibodies on G-UCNPs, forming G-UCNPs-MMP-8 conjugates on the conjugation pad (Fig. 9(D)). The migration of conjugates through the nitrocellulose (NC) membrane is facilitated by capillary force, leading to their capture by the MMP-8 capture antibodies (T line). This results in an antibody-antigen-antibody sandwich structure at the T line (Fig. 9(E)). The detection antibodies used in this study are generated from mice; it is expected that any surplus G-UCNP probes that fail to bind to the analytes will be captured by the goat anti-mouse IgG located on the C line. In the absence of an analyte within the sample, the probes will only bind to the goat anti-mouse IgG located on the C line. The luminescence signals on the G-UCNPs-LFIS are captured using a camera and afterward processed using Image J software for the concentration measurements.[134]

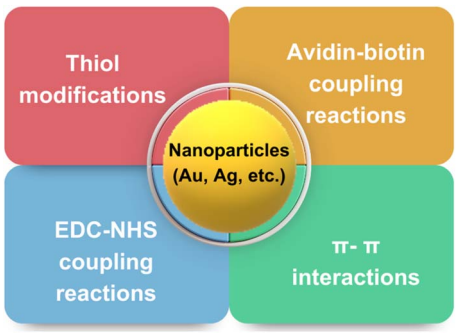

Fig. 10 Various strategies deployed routinely for surface modifications of nanoparticles.

A summary of recently reported LFAs with the colorimetric and fluorescence-based detection systems is given in Table 3. Such detection systems are suitable for low-resource settings and ideal for mass screening.

Apart from LFAs, colorimetric detection is an alternative for low-cost detection of oral cancer. As discussed earlier, colorimetric detection of oral cancer using ELISA was the most popular and widely used technique. However, low detection sensitivity, high costs, high-end laboratory settings, and longer

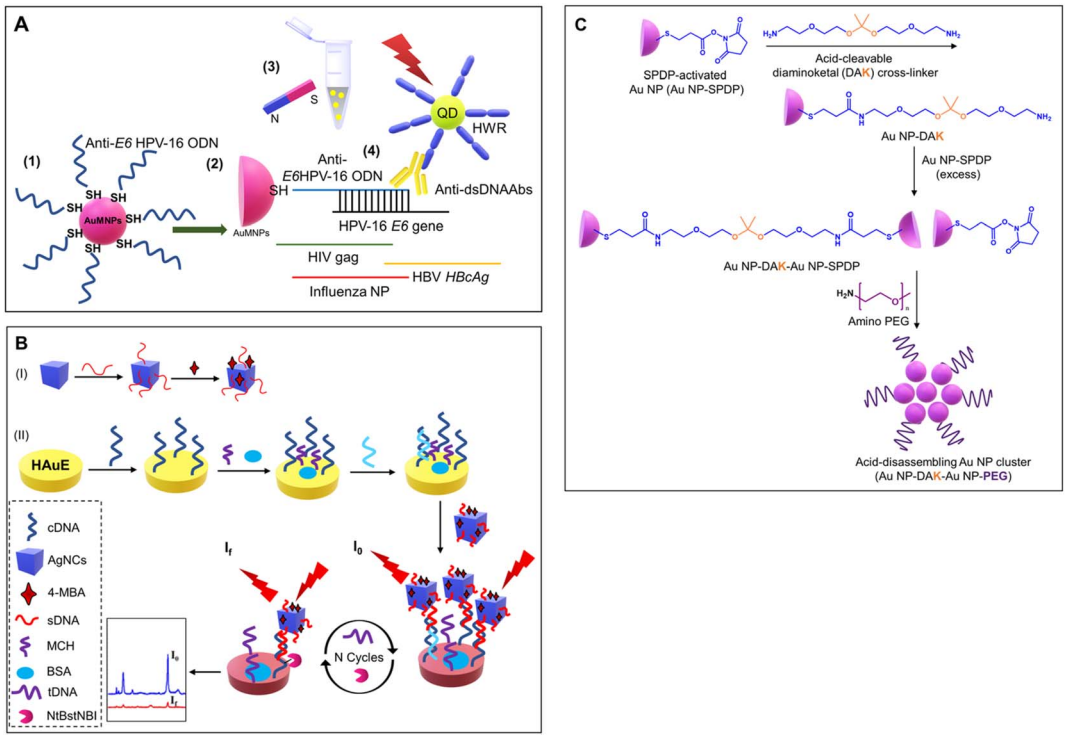

Fig. 11 (A) Schematic showing specific detection of HPV using functionalized gold nanoparticles and fluorescent QDs. Reproduced/re-drawn with permission from ref. 149. Copyright 2016 Elsevier B.V. (B) Figure illustrates the fabrication of a Ag-nanocube-based SERS biosensor for DNA detection. Reproduced/re-drawn with permission from ref. 151. Copyright 2021 Elsevier B.V. (C) Fabrication of acid-sensitive gold nanoclusters as a contrast agent for optical coherence tomography (OCT). Reproduced/re-drawn from ref. 150. Creative Commons license.

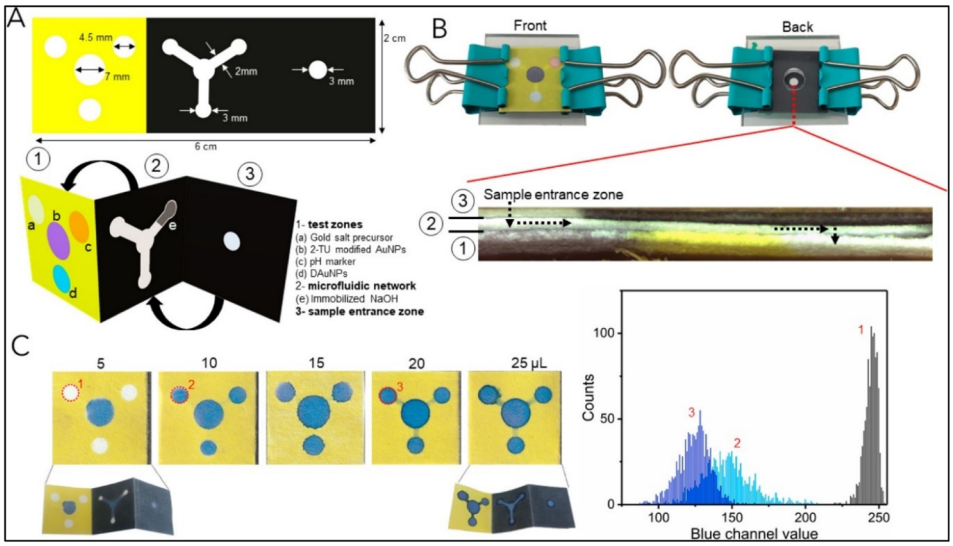

Fig. 12 The schematic of the device fabrication. (A) Dimension of the wax pattern used and other components: (1) test zones, (2) microfluidic network, and (3) sample entrance zone. The device is appropriately folded into a suitable conformation for inter-component interaction (B) The device is assembled by integrating it into the acrylic sheet and springs. A cross-sectional view of the device is presented to illustrate its configuration following the assembly process (sample flow is shown by a dashed arrow). (C) Flow assay to ascertain the minimal sample volume necessary for the device to function correctly. The graph shows a color histogram obtained from three separate test zones. Reproduced with permission from ref. 152. Copyright 2021 American Chemical Society.

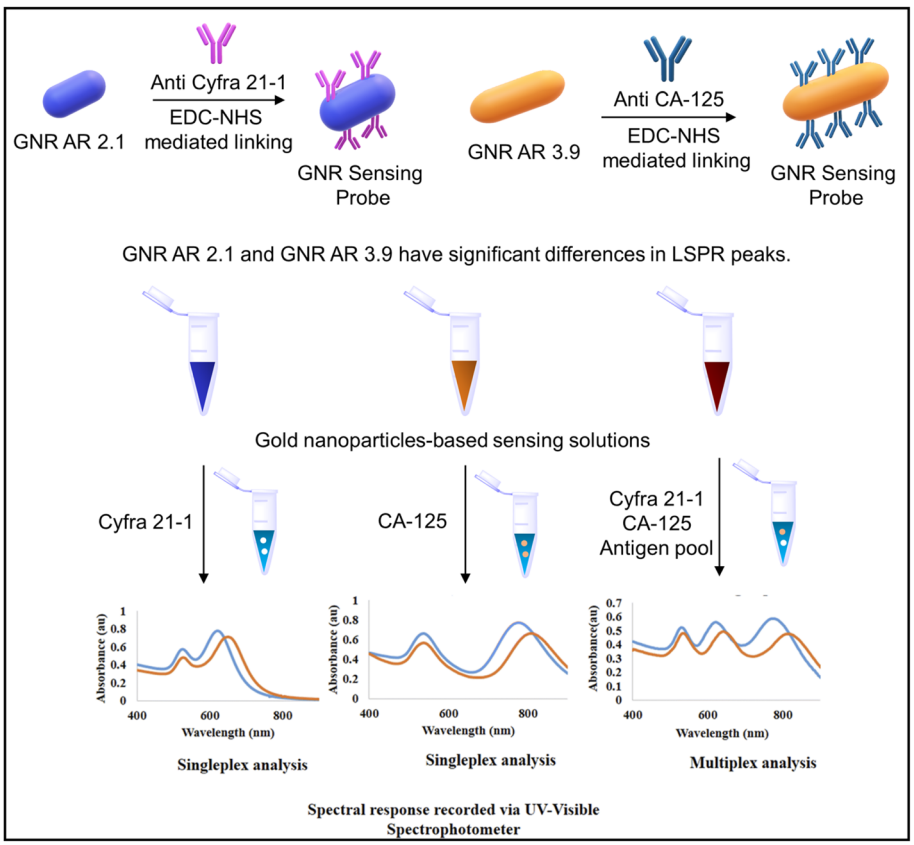

Fig. 13 The schematic depicting GNR probe development and the UV-visible spectroscopy-based spectral analysis of Cyfra 21-1 and CA-125 antigens. Reproduced/re-drawn with permission from ref. 153. Copyright 2022 The Royal Society of Chemistry.

experimental time are the limitations of the use of ELISA. However, gold and silver nanoparticles are highly explored for the development of various colorimetry-based assays for the detection of various biomarkers due to their surface plasmon resonance, high sensitivity, and ease of surface modification. The results can be interpreted using the basic principle of colorimetry. Thus, the following section discusses various gold and silver nanoparticle-based microfluidic detection systems.

8. Gold and silver nanoparticle-based sensors

Gold and silver nanoparticles are frequently used metallic nanoparticles in microfluidic systems. Nanoparticles typically serve as elements for capturing targets and/or transmitting signals, owing to their localized surface plasmon resonance (LSPR), catalytic activity, and conductivity. These nanoparticles are generally incorporated into the microfluidic systems using *in situ* synthesis or simply drop casting before or after mixing the analyte. These nanoparticles are also widely used in colorimetric detection using UV-vis spectroscopy.[7,143–147]

8.1. Functionalization of gold and silver nanoparticles

The critical factor in the use of gold and silver nanoparticles for point-of-care devices includes functionalization. The several well-established functionalization techniques include thiol modifications, EDC-NHS coupling reactions, avidin-biotin coupling reactions, and π- π interactions, as shown in

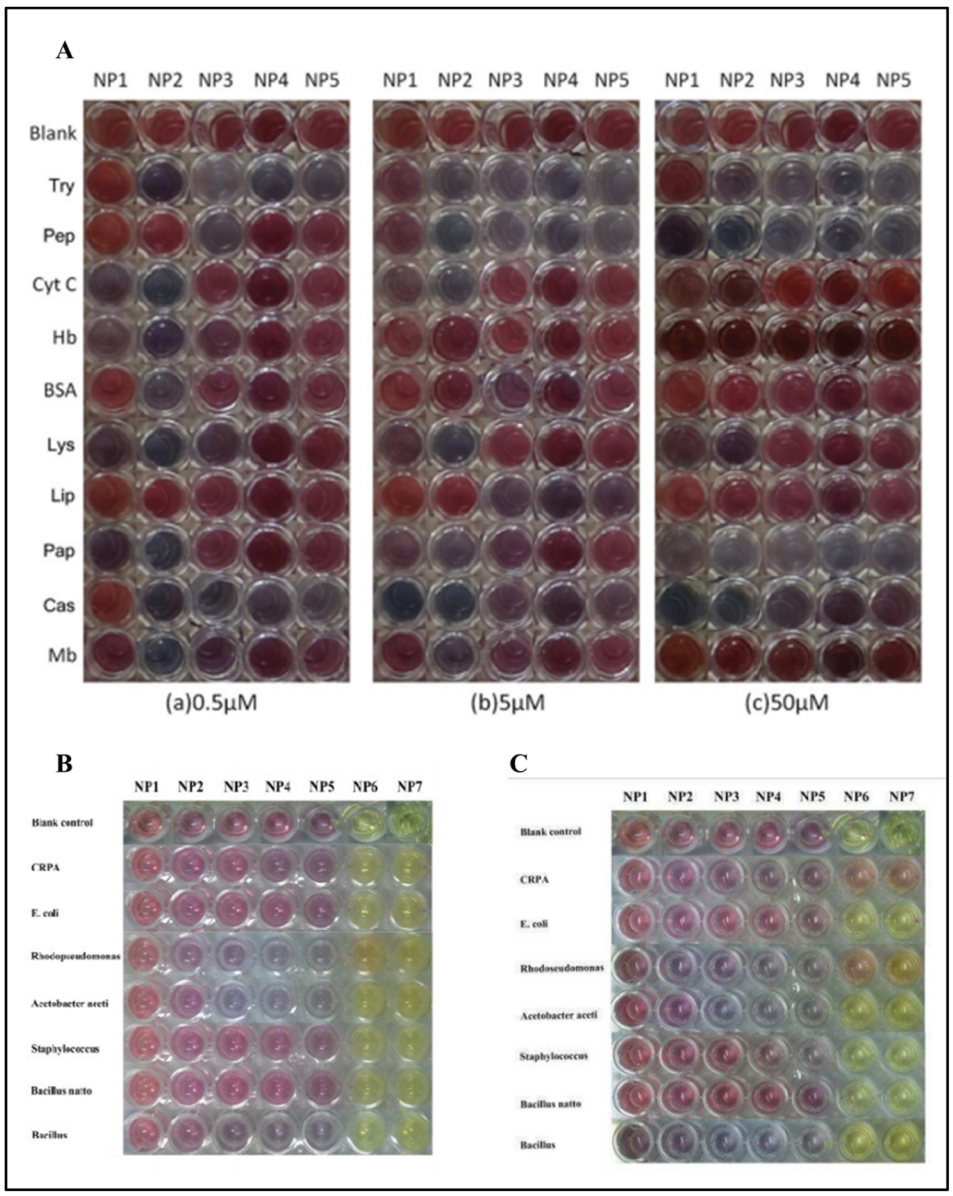

Fig. 14 (A) The picture shows the color pattern developed with gold nanoparticles with varying sizes upon interaction with different proteins. (B) The interaction of the gold nanoparticles and silver nanoparticles NP6 (25 nm) and NP7 (31 nm) against bacteria after 20 min; (C) after 6 hours. Reproduced with permission from ref. 156. Copyright 2015 The Royal Society of Chemistry.

Fig. 10.[148] These functionalization methods are used for the conjugation of antibodies for the respective detection of the antigens and are widely deployed strategies for specificity.

Here, a few gold and silver nanoparticle-based systems employed as a sensor *via* surface functionalization of nanoparticle surfaces are discussed. Jimenez *et al.* developed a gold nanoparticle-based detection system for the detection of human papillomavirus (HPV). The developed system consists of modified gold nanoparticles, with thiolated oligodeoxyribonucleotides consisting of the complementary sequence to the DNA sequence of the HPV oncogene and the modified CdTe quantum dots (QDs) for site-specific conjugation. The modified CdTe quantum dots act as a fluorescence tag in the detection system. The overall working principle is shown in Fig. 11(A).[149] In another study by Kim *et al.*, a stimuli-responsive contrast agent was developed for optical coherence tomography (OCT) using gold nanoparticles and acid-cleavable diaminoketal cross-linkers. It was shown that the developed contrast agent was able to detect early stage cancers (see Fig. 11(C)).[150] Due to multiplexed capacity and high sensitivity, surface-enhanced Raman scattering (SERS) has gained a lot of attention in biosensing. Liu *et al.* developed an Ag nanocube-based SERS system for the detection of oral cancer DNA. The silver nanocube surface was modified with signal DNA and 4-mercaptobenzoic acid as a Raman reporter. The cubic morphology of the deployed silver nanoparticles was able to produce a strong SERS signal. A heated gold electrode was also deployed in addition to functionalized silver nanocages to achieve amplification of the targeted DNA. The schematic of the sensor development is shown in Fig. 11(B).[151]

8.2. Low-cost gold/silver nanoparticle-based detection systems

The development of multiplex systems is of great interest in increasing the confidence level of disease diagnosis. Tomas Pinheiro *et al.* developed a gold nanoparticle-based colorimetric, non-enzymatic multiplex microfluidic paper-based detection system. The developed device was capable of detecting uric acid, cholesterol, and glucose. The limit of detection obtained was 1.25 mM, 71 μM, and 81 μM for glucose, uric acid, and cholesterol, respectively, which were comparable those of similar reported systems. The developed device was an example of a colorimetric, microfluidic, paper-based, non-enzymatic detection system. The schematic of the device fabrication is shown in Fig. 12.[152]

Another study using gold nanorods (GNRs) with varying aspect ratios (ARs) was performed by Debolina Chakraborty *et al.* for the multiplex colorimetry-based detection system of Cyfra 21-1 and CA-125. The designed assay could detect the mentioned biomarker in the salivary concentration range and was tested for artificial saliva. In this study, the antibodies targeting Cyfra 21-1 and CA-125 were utilized as probes to functionalize the gold nanorods with varying aspect ratios. The quantitative evaluation of the target analyte was assisted through antigen–antibody interactions that caused a spectrum shift of specific plasmon band maxima. The developed GNR probe could sense Cyfra 21-1 and CA-125 with a detection limit of 0.84 ng mL^{-1} and 1.6 U mL^{-1}, respectively. The study introduces a revolutionary nanoscale optical transducer technology that exhibits simplicity in design and implementation.

GNRs were modified with anti-Cyfra 21-1 and anti-CA-125 using EDC-NHS chemistry to detect the respective antigen from the artificial saliva samples. GNR probes were suitable for multiplex detection owing to their different aspect ratios and peak positions. This technology holds the potential for further development into miniaturized biochips suitable for low-resource settings.[153] The GNR probe development and analysis using UV-visible spectroscopy is shown in Fig. 13. In such a system, colorimetric detection can also be performed using low-cost portable optical detection systems ideal for mass screening in low-resource settings. Our group has developed several IoT-enabled portable colorimetry-based microfluidic detection systems.[154,155] Such devices with slight modifications

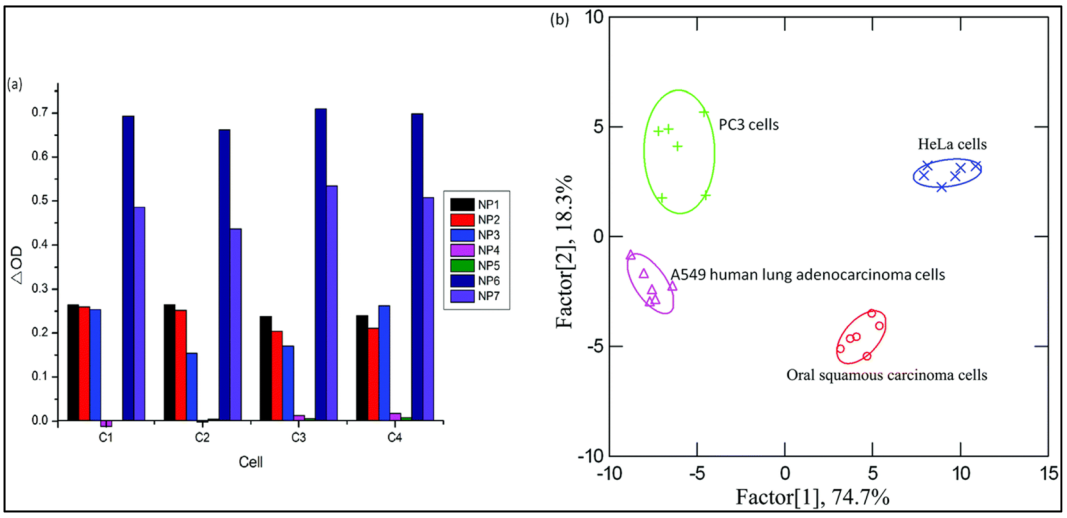

Fig. 15 The identification of various cancer cells. The absorbance pattern of seven nanoparticles against cancer cells (Left (a)) and the canonical score plot (Right (b)). Reproduced with permission from ref. 156. Copyright 2015 The Royal Society of Chemistry.

to the photodiode and a suitable light source (LED) of the required wavelength can be applied for a wide spectral range.

Dongyang Li *et al.* deployed gold and silver nanoparticles with different sizes. The diameters of the gold nanoparticles synthesized were 13, 25, 35, 50, and 60 nm, and for silver nanoparticles, the diameters were 25 and 31 nm to detect various proteins and bacteria without any functionalization of the nanoparticles. The developed colorimetric sensor arrays were tested for ten different proteins with 0.5, 5, and 50 μM concentrations. The proteins used in the study were cytochrome C (Cyt C), myoglobin (Mb), trypsin (Try), pepsin (Pep), lysozyme (Lys), papain (Pap), hemoglobin (Hb), casein (Cas), bovine serum albumin (BSA), and lipase (Lip). Seven types of bacteria were used as analytes, including CRPA, *Acetobacter aceti*, *Rhodopseudomonas*, *Bacillus natto*, *Staphylococcus*, *E. coli*, and Bacillus (see Fig. 14(B) and (C)). The types of cancer cells analyzed include OSCC cells, HeLa cells, PC3 cells, and A549 human lung adenocarcinoma cells.

Depending upon the protein's interaction type and the nanoparticles' size, a unique fingerprint color was obtained, which can be detected by linear discriminant analysis (LDA). The developed detection system could detect bacteria with a concentration of 0.05 OD in 200 μL. Interestingly, the array was also capable of the detection of cancer cells with a concentration of 5000 cells in 200 μL as shown in Fig. 15.[156]

9. Challenges and future perspectives

Colorimetry-based microfluidic devices have several benefits owing to the recent developments in the field and are an ideal solution for early oral cancer detection. However, several challenges remain, as discussed below and shown in Fig. 16.

In contemporary practice, saliva has emerged as a favored specimen for the purpose of oral cancer biomarker testing, surpassing alternative samples. This preference stems from the fact that saliva exhibits direct contact with lesions within the mouth cavity, its non-invasive nature, and its convenient collection process. Initially, it is imperative to comprehend the considerably diverse composition of saliva across various individuals. Furthermore, it is crucial to distinguish between oral inflammatory illnesses and other cancers since they may exhibit elevated levels of salivary biomarkers. This differentiation is crucial to enhance the sensitivity of salivary biomarker detection. Moreover, it is necessary to establish a standardized protocol for the saliva sample collection and storage as this will play a crucial role in the final analysis. Multiplexing is essential for accurate diagnosis. Nevertheless, the selection of an appropriate panel of biomarkers will effectively differentiate between various types of cancer and/or inflammatory disorders. This objective can be accomplished by extensively investigating a diverse range of positive samples obtained from individuals spanning different age groups, genders, and geographical locations.

The significance of paper-based microfluidic devices lies in their cost-effectiveness, portability, and simplified operation. Furthermore, the integration of diverse point-of-care devices with the Internet of Things (IoT) proves to be advantageous for conducting screenings in remote regions where the availability of advanced laboratory facilities is limited. Paper-based systems do not possess precise mechanisms for concentration detection. Multiplexing is another crucial aspect that warrants consideration. The device should be able to concurrently identify and quantify many biomarkers from a single, relatively modest sample. In addition, most paper-based devices utilize a range of antibodies and other biomolecules, raising concerns regarding their storage, transportation, and shelf-life.

Lastly, artificial intelligence (AI) and machine learning (ML) aided technologies should be extensively developed and deployed for massive data analysis and for early oral cancer diagnosis.

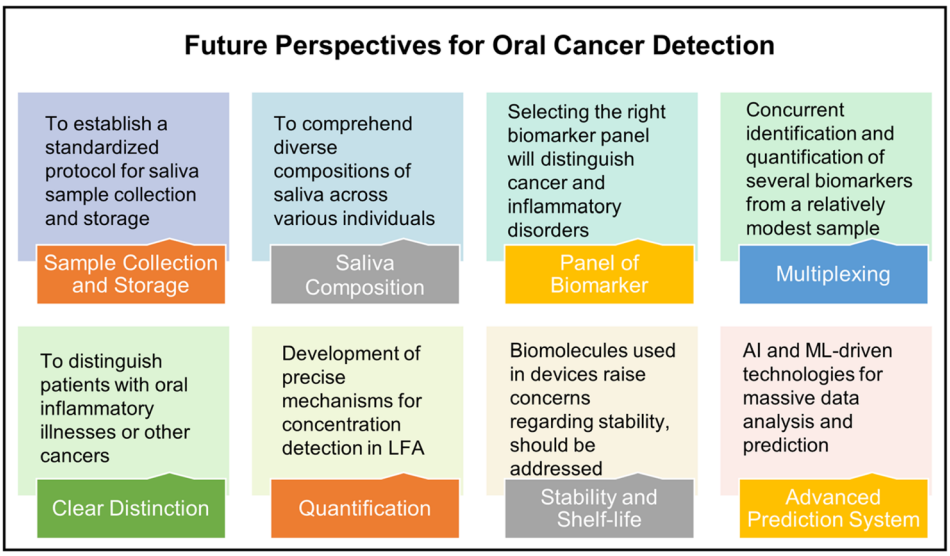

Fig. 16 Schematic showing future perspectives for oral cancer detection using colorimetry-based microfluidic devices and salivary biomarkers.

10. Conclusion

The present study examines a range of salivary biomarkers that are known to exhibit substantial alterations in concentration in oral malignancies. The discussion has extensively covered several salivary biomarkers, examining their structure and importance in the early identification and progression of oral cancer. As elucidated in the review above, the salivary biomarkers under consideration exhibit considerable promise in the early identification of oral cancer and monitoring disease advancement. Nevertheless, it is essential to note that the identification of oral cancer cannot be reliably achieved using a single biomarker. This is because numerous biomarkers have been observed to exhibit alterations in various types of malignancies, as well as some other medical disorders. Multiplex detection is a reliable method for early detection, offering advantages such as specificity, precision, and high levels of confidence. The conventional gold standard ELISA method has several drawbacks, such as expensive text kits requiring highly skilled technicians, laboratory settings, and high detection time. Multiplexing with the ELISA is another challenge. The incorporation of microfluidics as a platform in many biosensors has facilitated enhanced automation capabilities, simplified multiplexing, and reduced processing durations, and enabled high-throughput analysis. Utilizing paper-based microfluidics to identify salivary biomarkers effectively represents a facile, economical, and portable approach to developing new biosensors. Paper-based microfluidics are highly suitable for low-resource settings due to their adherence to the REASSURED criteria outlined by the World Health Organization. LFAs and paper-based low-cost devices working on various detection systems have been discussed in detail. Such low-cost devices with high accuracy and detection precision can be deployed for mass screening for early diagnosis.

Data availability

No primary research results, software, or code have been included, and no new data were generated or analyzed in this review.

Author contributions

Aniket Balapure: conceptualization, data curation, formal analysis, investigation, writing – original draft. Satish Kumar Dubey: funding acquisition, project administration, supervision, writing – reviewing and editing. Arshad Javed: funding acquisition, project administration, supervision, writing – reviewing and editing. Samit Chattopadhyay: funding acquisition, project administration, supervision, writing – reviewing and editing. Sanket Goel: funding acquisition, project administration, supervision, writing – reviewing and editing.

Conflicts of interest

The authors declare that they have no known competing financial interests or personal relationships that could have appeared to influence the work reported in this paper.

Acknowledgements

This work was supported by the BITS BioCyTiH Foundation, India [BBF/BITS(G)/FY2022-23/BCPS-110]. A. B. would like to thank the BITS BioCyTiH Foundation, India for fellowship support.

References

1 E. Nakamichi, H. Sakakura, S. Mii, N. Yamamoto, H. Hibi, M. Asai and M. Takahashi, *Oral Dis.*, 2021, **27**, 439–447.
2 N. J. D'Silva, C. Perez-Pacheco and L. B. Schmitd, *Adv. Biol.*, 2023, 7.
3 S. Chupradit, S. A. Jasim, D. Bokov, M. Z. Mahmoud, A. B. Roomi, K. Hachem, M. Rudiansyah, W. Suksatan and R. Bidares, *Anal. Methods*, 2022, **14**, 1301–1310.
4 O. J. Old, L. M. Fullwood, R. Scott, G. R. Lloyd, L. M. Almond, N. A. Shepherd, N. Stone, H. Barr and C. Kendall, *Anal. Methods*, 2014, **6**, 3901–3917.
5 S. Verma, A. Singh, A. Shukla, J. Kaswan, K. Arora, J. Ramirez-Vick, P. Singh and S. P. Singh, *ACS Appl. Mater. Interfaces*, 2017, **9**, 27462–27474.
6 B. L. Ziober, M. G. Mauk, E. M. Falls, Z. Chen, A. F. Ziober and H. H. Bau, *Head Neck*, 2008, **30**, 111–121.
7 Y. Xiang, C. Hu, G. Wu, S. Xu and Y. Li, *TrAC, Trends Anal. Chem.*, 2023, **158**, 116835.
8 V. Borse, A. N. Konwar and P. Buragohain, *Sens. Int.*, 2020, **1**, 100046.
9 S. C. Chang, W. L. Lin, Y. F. Chang, C. T. Lee, J. S. Wu, P. H. Hsu and C. F. Chang, *J. Food Drug Anal.*, 2019, **27**, 483–493.
10 Y. W. Lin, S. T. Huang, J. C. Wu, T. H. Chu, S. C. Huang, C. C. Lee and M. H. Tai, *BMC Cancer*, 2019, **19**, 1083.
11 Y. T. Chang, L. J. Chu, Y. C. Liu, C. J. Chen, S. F. Wu, C. H. Chen, I. Y. F. Chang, J. S. Wang, T. Y. Wu, S. Dash, W. F. Chiang, S. F. Chiu, S. B. Gou, C. Y. Chien, K. P. Chang and J. S. Yu, *Cancers*, 2020, **12**, 2273.
12 A. Manz, E. Verpoorte, D. E. Raymond, C. S. Effenhauser, N. Burggraf and H. M. Widmer, *Micro Total Analysis Systems*, ed. A. Van den Berg and P. Bergveld, Springer Netherlands, Dordrecht, 1995, pp. 5–27.
13 B. D. Cardoso, E. M. S. Castanheira, S. Lanceros-Mendez and V. F. Cardoso, *Adv. Healthcare Mater.*, 2023, 2202936.
14 E. Solhi, M. Hasanzadeh and P. Babaie, *Anal. Methods*, 2020, **12**, 1398–1414.
15 H. A. Silva-Neto, I. V. S. Arantes, A. L. Ferreira, G. H. M. do Nascimento, G. N. Meloni, W. R. de Araujo, T. R. L. C. Paixao and W. K. T. Coltro, *Trends Anal. Chem.*, 2023, **158**, 116893.
16 A. Kumar, D. Jain, J. Bahuguna, M. Bhaiyya, S. K. Dubey, A. Javed and S. Goel, *Biosens. Bioelectron.*, 2023, **238**, 115582.
17 M. L. Bhaiyya, S. K. Srivastava, P. K. Pattnaik and S. Goel, *IEEE Trans. Instrum. Meas.*, 2023, **72**, 1–8.
18 J. M. Mohan, S. Kumar, K. Amreen, A. Javed, S. K. Dubey and S. Goel, *IEEE Sens. J.*, 2023, **23**, 16189–16196.

19 M. Sharafeldin, T. Chen, G. U. Ozkaya, D. Choudhary, A. A. Molinolo, J. S. Gutkind and J. F. Rusling, *Biosens. Bioelectron.*, 2021, **171**, 112681.
20 F. Wehrhan, M. Weber, C. Baran, A. Agaimy, M. Buttner-Herold, M. Kesting and J. Ries, *J. Cranio-Maxillofacial Surg.*, 2021, **49**, 118–125.
21 X. Zhang and B. Li, *Oral Dis.*, 2023, **29**, 51–61.
22 M. Hasanzadeh, N. Shadjou and M. de la Guardia, *Trends Anal. Chem.*, 2017, **91**, 125–137.
23 K. E. Kaczor-Urbanowicz, F. Wei, S. L. Rao, J. Kim, H. Shin, J. Cheng, M. Tu, D. T. W. Wong and Y. Kim, *Biochim. Biophys. Acta Rev. Canc.*, 2019, **1872**, 49–59.
24 D. Kademani, *Mayo Clin. Proc.*, 2007, **82**, 878–887.
25 M. Zhao, C. Ji, H. Dai, C. Wang, R. Liu, J. Xie, Y. Wang and Z. Gu, *ACS Appl. Mater. Interfaces*, 2023, **15**, 4984–4995.
26 K. Mahato, A. Kumar, P. K. Maurya and P. Chandra, *Biosens. Bioelectron.*, 2018, **100**, 411–428.
27 O. Hershkovich, I. Shafat and R. M. Nagler, *J. Gerontol., Ser. A*, 2007, **62**, 361–366.
28 B. N. Kallalli, K. Rawson, Muzammil, A. Singh, M. A. Awati and P. Shivhare, *J. Oral Pathol. Med.*, 2016, **45**, 687–690.
29 W. Jin, M. Zhu, Y. Zheng, Y. Wu, X. Ding, H. Wu, J. Ye, Y. Wu, Z. Zhu and X. Song, *Oral Dis.*, 2022, **28**, 132–141.
30 T. P. Mafessoni, C. E. Mazur and J. M. Amenabar, *Med. Hypotheses*, 2018, **119**, 29–31.
31 M. Moradi Binabaj, A. Bahrami, M. Khazaei, M. Ryzhikov, G. A. Ferns, A. Avan and S. Mahdi Hassanian, *Gene*, 2020, **728**, 144283.
32 A. Pecoraro, P. Carotenuto, G. Russo and A. Russo, *Sci. Rep.*, 2019, **9**, 15431.
33 S. Manna, R. Kirtana, A. Roy, T. Baral and S. K. Patra, *Arch. Biochem. Biophys.*, 2023, **742**, 109600.
34 J. Kaur, M. Preethi, R. Srivastava and V. Borse, *Biosens. Bioelectron.: X*, 2022, **11**, 100212.
35 L. Zhong, C. Zhang, J. Zheng, J. Li, W. Chen and Z. Zhang, *Arch. Oral Biol.*, 2007, **52**, 1079–1087.
36 K. Rajkumar, R. Ramya, G. Nandhini, P. Rajashree, A. Ramesh Kumar and S. Nirmala Anandan, *Oral Dis.*, 2015, **21**, 90–96.
37 S. S. Sawant, D. A. Chaukar, S. S. Joshi, P. P. Dange, S. Kannan, S. Kane, A. K. D'Cruz and M. M. Vaidya, *Oral Oncol.*, 2011, **47**, 114–120.
38 S. S. Sawant, S. M. Zingde and M. M. Vaidya, *Oral Oncol.*, 2008, **44**, 722–732.
39 P. Panta and D. T. W. Wong, *Oral Cancer Detection: Novel Strategies and Clinical Impact*, ed. P. Panta, Springer International Publishing, Cham, 2019, pp. 265–295.
40 T. I. Goonewardene, M. R. Hall and G. J. S. Rustin, *Lancet Oncol.*, 2007, **8**, 813–821.
41 S. Scarà, P. Bottoni and R. Scatena, *Advances in Cancer Biomarkers: from Biochemistry to Clinic for a Critical Revision*, ed. R. Scatena, Springer Netherlands, Dordrecht, 2015, pp. 247–260.
42 R. M. Nagler, *Oral Oncol.*, 2009, **45**, 1006–1010.
43 N. Shahbazi, S. Hosseinkhani and B. Ranjbar, *Sens. Actuators, B*, 2017, **253**, 794–803.
44 Y. Li, S. Hu, C. Chen, N. Alifu, X. Zhang, J. Du, C. Li, L. Xu, L. Wang and B. Dong, *Talanta*, 2023, **258**, 124435.
45 L. Yen, C. Kao and S. Wang, *Clin. Otolaryngol. Allied Sci.*, 1998, **23**, 82–86.
46 H. Zhu, *Diagnostics*, 2022, **12**, 1065.
47 M. Yang, J. Ding, Q. Luo, X. Chen and F. Chen, *Clin. Chim. Acta*, 2022, **525**, 40–45.
48 V. Tumuluri, G. A. Thomas and I. S. Fraser, *J. Oral Pathol. Med.*, 2002, **31**, 598–604.
49 R. Patruno, N. Zizzo, A. F. Zito, V. Catalano, P. Valerio, V. Pellecchia, E. D'errico, F. Mazzone, P. D. Ribatti and G. Ranieri, *Leuk. Lymphoma*, 2006, **47**, 1138–1143.
50 M. A. Gonzalez-Moles, I. Ruiz-Avila, J. A. Gil-Montoya, F. Esteban and M. Bravo, *Oral Oncol.*, 2010, **46**, 525–530.
51 C. J. Barnes, K. Ohshiro, S. K. Rayala, A. K. El Naggar and R. Kumar, *Clin. Cancer Res.*, 2007, **13**, 4291–4299.
52 F. Hofmann and C. Garcia-Echeverria, *Drug Discov. Today*, 2005, **10**, 1041–1047.
53 A. Knuppel, G. K. Fensom, E. L. Watts, M. J. Gunter, N. Murphy, K. Papier, A. Perez-Cornago, J. A. Schmidt, K. Smith Byrne, R. C. Travis and T. J. Key, *Cancer Res.*, 2020, **80**, 4014–4021.
54 B. P. Patel, P. M. Shah, U. M. Rawal, A. A. Desai, S. V Shah, R. M. Rawal and P. S. Patel, *J. Surg. Oncol.*, 2005, **90**, 81–88.
55 R. D. Singh, N. Haridas, J. B. Patel, F. D. Shah, S. N. Shukla, P. M. Shah and P. S. Patel, *Indian J. Clin. Biochem.*, 2010, **25**, 250–259.
56 T. Shpitzer, Y. Hamzany, G. Bahar, R. Feinmesser, D. Savulescu, I. Borovoi, M. Gavish and R. M. Nagler, *Br. J. Cancer*, 2009, **101**, 1194–1198.
57 J. Kaur, R. Jacobs, Y. Huang, N. Salvo and C. Politis, *Clin. Oral Invest.*, 2018, **22**, 633–640.
58 Z. Khurshid, M. S. Zafar, R. S. Khan, S. Najeeb, P. D. Slowey and I. U. Rehman, Chapter Two - Role of Salivary Biomarkers in Oral Cancer Detection, *Advances in Clinical Chemistry*, ed. G. S. Makowski, Elsevier, 2018, vol. 86, pp. 23–70.
59 Y. S. L. Cheng, T. Rees and J. Wright, *Clin. Transl. Med.*, 2014, **3**, 3.
60 P. Kumar, S. Gupta and B. C. Das, *Transl. Oncol.*, 2024, **40**, 101827.
61 O. Barros, V. G. D'Agostino, L. Lara Santos, R. Vitorino and R. Ferreira, *Expert Rev. Proteomics*, 2024, **21**, 149–168.
62 J. Wang, J. Jing, C. Zhou and Y. Fan, *Int. J. Oral Sci.*, 2024, **16**, 4.
63 A. Radaic, P. Kamarajan, A. Cho, S. Wang, G. C. Hung, F. Najarzadegan, D. T. Wong, H. Ton-That, C. Y. Wang and Y. L. Kapila, *Periodontology*, 2000, **2023**, 01–31.
64 V. R. Umapathy, P. M. Natarajan and B. Swamikannu, *Molecules*, 2023, **28**, 5283.
65 P. Dongiovanni, M. Meroni, S. Casati, R. Goldoni, D. V. Thomaz, N. S. Kehr, D. Galimberti, M. Del Fabbro and G. M. Tartaglia, *Int. J. Oral Sci.*, 2023, **15**, 27.
66 Y. Zhou and Z. Liu, *Clin. Chim. Acta*, 2023, **548**, 117503.
67 R. Goldoni, A. Scolaro, E. Boccalari, C. Dolci, A. Scarano, F. Inchingolo, P. Ravazzani, P. Muti and G. Tartaglia, *Biosensors*, 2021, **11**, 396.

68 J. Adeoye, P. A. Brennan and P. Thomson, *J. Oral Pathol. Med.*, 2020, **49**, 711–719.
69 R. Nagler, G. Bahar, T. Shpitzer and R. Feinmesser, *Clin. Cancer Res.*, 2006, **12**, 3979–3984.
70 T. Shpitzer, G. Bahar, R. Feinmesser and R. M. Nagler, *J. Cancer Res. Clin. Oncol.*, 2007, **133**, 613–617.
71 G. Bahar, R. Feinmesser, T. Shpitzer, A. Popovtzer and R. M. Nagler, *Cancer*, 2007, **109**, 54–59.
72 J. Balakittnen, C. Ekanayake Weeramange, D. F. Wallace, P. H. G. Duijf, A. S. Cristino, G. Hartel, R. A. Barrero, T. Taheri, L. Kenny, S. Vasani, M. Batstone, O. Breik and C. Punyadeera, *Int. J. Oral Sci.*, 2024, **16**, 14.
73 H. A. A. Alafaria and A. S. Jalal, *J. Appl. Genet.*, 2024, 1–8.
74 L. J. Chu, Y. T. Chang, C. Y. Chien, H. C. Chung, S. F. Wu, C. J. Chen, Y. C. Liu, W. C. Liao, C. H. Chen, W. F. Chiang, K. P. Chang, J. S. Wang and J. S. Yu, *Biomed. J.*, 2024, **47**, 100594.
75 S. K. Ghosh, Y. Man, A. Fraiwan, C. Waters, C. McKenzie, C. Lu, D. Pfau, H. Kawsar, N. Bhaskaran, P. Pandiyan, G. Jin, F. Briggs, C. C. Zender, R. Rezaee, F. Panagakos, J. E. Thuener, J. Wasman, A. Tang, H. Qari, T. Wise-Draper, T. S. McCormick, A. Madabhushi, U. A. Gurkan and A. Weinberg, *Cell Rep. Med.*, 2024, **5**, 101447.
76 J. Zheng, K. Chen, L. Cai, Y. Pan and Y. Zeng, *J. Cancer*, 2024, **15**, 1593.
77 A. Jain, A. A. Khan, R. Kaur, R. K. Verma, J. Bakshi, A. Chatterjee, A. Bal, S. Ghoshal and A. Pal, *Oral Oncol. Rep.*, 2024, **10**, 100478.
78 R. Shalaby, S. Ibrahim, A. A. W. Kotb, S. Baz, L. Hafed, O. Shaker and S. Afifi, *Oral Dis.*, 2024, **30**, 2075–2083.
79 A. Patel, S. Patel, P. Patel, D. Mandlik, K. Patel and V. Tanavde, *Int. J. Mol. Sci.*, 2022, **23**, 10639.
80 C. I. Faur, R. C. Roman, A. Jurj, L. Raduly, O. Almaşan, H. Rotaru, M. Chirila, M. A. Moldovan, M. Hedesiu and C. Dinu, *Medicina*, 2022, **58**, 1478.
81 L. He, F. Ping, Z. Fan, C. Zhang, M. Deng, B. Cheng and J. Xia, *Biomed. Pharmacother.*, 2020, **121**, 109553.
82 M. Honarmand, R. Saravani, L. Farhad-Mollashahi and A. Smailpoor, *Int. J. Cancer Manag.*, 2021, **14**, e108344.
83 Y. T. Chang, L. J. Chu, Y. C. Liu, C. J. Chen, S. F. Wu, C. H. Chen, I. Y. F. Chang, J. S. Wang, T. Y. Wu, S. Dash, W. F. Chiang, S. F. Chiu, S. B. Gou, C. Y. Chien, K. P. Chang and J. S. Yu, *Cancers*, 2020, **12**, 2273.
84 P. C. B. Faria, A. P. Carneiro, R. Binato, R. Nascimento, P. S. Santos, D. Fagundes, S. J. da Silva, A. M. Loyola, E. Abdelhay and L. R. Goulart, *Sci. Rep.*, 2019, **9**, 18399.
85 S. Langevin, D. Kuhnell, T. Parry, J. Biesiada, S. Huang, T. Wise-Draper, K. Casper, X. Zhang, M. Medvedovic and S. Kasper, *Oncotarget*, 2017, **8**, 82459.
86 R. Metgud and S. Bajaj, *Biotech. Histochem.*, 2016, **91**, 96–101.
87 J. Wei, G. Xie, Z. Zhou, P. Shi, Y. Qiu, X. Zheng, T. Chen, M. Su, A. Zhao and W. Jia, *Int. J. Cancer*, 2011, **129**, 2207–2217.
88 D. J. Patil and C. B. More, *J. Oral Maxillofac. Surg. Med. Pathol.*, 2021, **33**, 546–554.
89 E. Hyvarinen, B. Kashyap and A. M. Kullaa, *Metabolites*, 2023, **13**, 498.
90 S. Ishikawa, M. Sugimoto, K. Kitabatake, A. Sugano, M. Nakamura, M. Kaneko, S. Ota, K. Hiwatari, A. Enomoto, T. Soga, M. Tomita and M. Iino, *Sci. Rep.*, 2016, **6**, 31520.
91 M. Yuvaraj, K. Udayakumar, V. Jayanth, A. Prakasa Rao, G. Bharanidharan, D. Koteeswaran, B. D. Munusamy, C. Murali krishna and S. Ganesan, *J. Photochem. Photobiol., B*, 2014, **130**, 153–160.
92 J. Vimal, N. A. George, R. R. Kumar, J. Kattoor and S. Kannan, *Arch. Oral Biol.*, 2023, **155**, 105780.
93 K. Tzimas and E. Pappa, *Metabolites*, 2023, **13**, 379.
94 C. Liao, X. Chen and Y. Fu, *Interdiscip. Med.*, 2023, **1**, e20230009.
95 N. Chuchueva, F. Carta, H. N. Nguyen, J. Luevano, I. A. Lewis, I. Rios-Castillo, V. Fanos, E. King, V. Swistushkin, I. Reshetov, Y. Rusetsky, K. Shestakova, N. Moskaleva, C. Mariani, A. Castillo-Carniglia, D. Grapov, J. Fahrmann, M. R. La Frano, R. Puxeddu, S. A. Appolonova and A. Brito, *Metabolomics*, 2023, **19**, 77.
96 S. Alapati, G. Fortuna, G. Ramage and C. Delaney, *Metabolites*, 2023, **13**, 890.
97 G. Luo, S. Wang, W. Lu, W. Ju, J. Li, X. Tan, H. Zhao, W. Han and X. Yang, *Oral Dis.*, 2024, 1–13.
98 S. Ishikawa, M. Sugimoto, K. Kitabatake, M. Tu, A. Sugano, I. Yamamori, A. Iba, K. Yusa, M. Kaneko, S. Ota, K. Hiwatari, A. Enomoto, T. Masaru and M. Iino, *Amino Acids*, 2017, **49**, 761–770.
99 S. Wang, M. Yang, R. Li and J. Bai, *Eur. J. Med. Res.*, 2023, **28**, 53.
100 K. Honigova, J. Navratil, B. Peltanova, H. H. Polanska, M. Raudenska and M. Masarik, *Biochim. Biophys. Acta Rev. Canc.*, 2022, **1877**, 188705.
101 S. Jagadeeshan, O. Z. Novoplansky, O. Cohen, I. Kurth, J. Hess, A. J. Rosenberg, J. R. Grandis and M. Elkabets, *Biochim. Biophys. Acta Rev. Canc.*, 2023, **1878**, 188963.
102 K. Omura, *Int. J. Clin. Oncol.*, 2014, **19**, 423–430.
103 S. H. Huang, E. Hahn, S. I. Chiosea, Z. Y. Xu, J. S. Li, L. Shen and B. O'Sullivan, *Oral Oncol.*, 2020, **102**, 104563.
104 Y. Xiao, L. Mao, Q. C. Yang, S. Wang, Z. Z. Wu, S. C. Wan, M. J. Zhang and Z. J. Sun, *Oral Oncol.*, 2023, **138**, 106331.
105 M. Boccellino, A. De Rosa and M. Di Domenico, *Diagnostics*, 2023, **13**, 2001.
106 J. Saini, J. Bakshi, N. K. Panda, M. Sharma, A. K. Yadav, K. Kamboj and A. K. Goyal, *J. Maxillofac. Oral Surg.*, 2023, 1–10.
107 D. Chakraborty, T. S. Viveka, K. Arvind, V. Shyamsundar, M. Kanchan, S. A. Alex, N. Chandrasekaran, R. Vijayalakshmi and A. Mukherjee, *Clin. Chim. Acta*, 2018, **477**, 166–172.
108 M. E. Arellano-Garcia, S. Hu, J. Wang, B. Henson, H. Zhou, D. Chia and D. T. Wong, *Oral Dis.*, 2008, **14**, 705–712.
109 M. S. Tabatabaei, R. Islam and M. Ahmed, *Anal. Chim. Acta*, 2021, **1143**, 250–266.

110 Y. T. Lin, S. Darvishi, A. Preet, T. Y. Huang, S. H. Lin, H. H. Girault, L. Wang and T. E. Lin, *Chemosensors*, 2020, **8**, 54.
111 H. Andersson and A. van den Berg, *Sens. Actuators, B*, 2003, **92**, 315–325.
112 B. K. Nahak, A. Mishra, S. Preetam and A. Tiwari, *ACS Appl. Bio Mater.*, 2022, **5**, 3576–3607.
113 J. Shoji, R. P. Davis, C. L. Mummery and S. Krauss, *Adv. Healthcare Mater.*, 2023, 2301067.
114 A. G. Monteduro, S. Rizzato, G. Caragnano, A. Trapani, G. Giannelli and G. Maruccio, *Biosens. Bioelectron.*, 2023, **231**, 115271.
115 H. Kutluk, E. E. Bastounis and I. Constantinou, *Adv. Healthcare Mater.*, 2023, **12**, 2203256.
116 L. Sun, F. Bian, D. Xu, Y. Luo, Y. Wang and Y. Zhao, *Mater. Horiz.*, 2023, **10**, 4724–4745.
117 M. Keuper-Navis, M. Walles, B. Poller, A. Myszczyszyn, T. K. van der Made, J. Donkers, H. Eslami Amirabadi, M. J. Wilmer, S. Aan, B. Spee, R. Masereeuw and E. van de Steeg, *Pharmacol. Res.*, 2023, **195**, 106853.
118 S. Rahmani Dabbagh, M. Rezapour Sarabi, M. T. Birtek, N. Mustafaoglu, Y. S. Zhang and S. Tasoglu, *Aggregate*, 2023, **4**, e197.
119 A. R. Ahmed, O. C. Gauntlett and G. Camci-Unal, *ACS Omega*, 2021, **6**, 46–54.
120 T. Mahmoudi, M. de la Guardia and B. Baradaran, *Trends Anal. Chem.*, 2020, **125**, 115842.
121 J. A. Otoo and T. S. Schlappi, *Biosensors*, 2022, **12**, 124.
122 K. J. Land, D. I. Boeras, X.-S. Chen, A. R. Ramsay and R. W. Peeling, *Nat. Microbiol.*, 2019, **4**, 46–54.
123 A. A. Shalaby, C. W. Tsao, A. Ishida, M. Maeki and M. Tokeshi, *Sens. Actuators, B*, 2023, **379**, 133243.
124 M. K. Dey, M. Iftesum, R. Devireddy and M. R. Gartia, *Anal. Methods*, 2023, **15**, 4351–4376.
125 E. Gumus, H. Bingol and E. Zor, *J. Pharm. Biomed. Anal.*, 2023, **225**, 115206.
126 R. Gupta, P. Gupta, S. Wang, A. Melnykov, Q. Jiang, A. Seth, Z. Wang, J. J. Morrissey, I. George, S. Gandra, P. Sinha, G. A. Storch, B. A. Parikh, G. M. Genin and S. Singamaneni, *Nat. Biomed. Eng.*, 2023, **7**, 1556–1570.
127 W. He, M. Wang, P. Cheng, Y. Liu and M. You, *Trends Anal. Chem.*, 2024, **176**, 117735.
128 T. Mahmoudi, M. de la Guardia and B. Baradaran, *Trends Anal. Chem.*, 2020, **125**, 115842.
129 E. B. Bahadır and M. K. Sezginturk, *Trends Anal. Chem.*, 2016, **82**, 286–306.
130 K. Khachornsakkul, W. Dungchai and N. Pamme, *ACS Sens.*, 2022, **7**, 2410–2419.
131 Z. Li, Q. Liu, Y. Li, W. Yuan and F. Y. Li, *J. Rare Earths*, 2021, **39**, 11–18.
132 W. Li, W. Peng, Y. Zhang, P. Liu, X. Gong, H. Liu and J. Chang, *Anal. Chim. Acta*, 2022, **1221**, 340112.
133 S. Wen, J. Zhou, K. Zheng, A. Bednarkiewicz, X. Liu and D. Jin, *Nat. Commun.*, 2018, **9**, 2415.
134 W. He, M. You, Z. Li, L. Cao, F. Xu, F. Li and A. Li, *Sens. Actuators, B*, 2021, **334**, 129673.
135 Y. Wang, Q. Chen, Y. Wang, F. Tu, X. Chen, J. Li and Z. Liu, *Talanta*, 2023, **256**, 124317.
136 O. Mukama, W. Wu, J. Wu, X. Lu, Y. Liu, Y. Liu, J. Liu and L. Zeng, *Talanta*, 2020, **210**, 120624.
137 V. Ranganathan, S. Srinivasan, A. Singh and M. C. DeRosa, *Anal. Biochem.*, 2020, **588**, 113471.
138 Z. Li, H. Chen and P. Wang, *Analyst*, 2019, **144**, 3314–3322.
139 Z. Yang, C. Yi, S. Lv, Y. Sheng, W. Wen, X. Zhang and S. Wang, *Sens. Actuators, B*, 2019, **285**, 326–332.
140 C. Gui, K. Wang, C. Li, X. Dai and D. Cui, *Nanoscale Res. Lett.*, 2014, **9**, 57.
141 O. Mukama, T. Yuan, Z. He, Z. Li, J. de Dieu Habimana, M. Hussain, W. Li, Z. Yi, Q. Liang and L. Zeng, *Sens. Actuators, B*, 2020, **316**, 128119.
142 W. Z. Lin, I. C. Ma, J. P. Wang, P. C. Hsieh, C. C. Liu and S. Y. Hou, *Anal. Bioanal. Chem.*, 2021, **413**, 2235–2246.
143 Y. Hang, A. Wang and N. Wu, *Chem. Soc. Rev.*, 2024, **53**, 2932–2971.
144 F. Beck, M. Loessl and A. J. Baeumner, *Microchim. Acta*, 2023, **190**, 91.
145 N. C. Dalibera, A. F. Oliveira and A. R. Azzoni, *Microfluid. Nanofluidics*, 2023, **27**, 56.
146 F. Hou, S. Sun, S. W. Abdullah, Y. Tang, X. Li and H. Guo, *Anal. Methods*, 2023, **15**, 2154–2180.
147 P. Nath and A. Ray, *Curr. Opin. Biomed. Eng.*, 2023, **28**, 100504.
148 R. Shandilya, A. Bhargava, N. Bunkar, R. Tiwari, I. Y. Goryacheva and P. K. Mishra, *Biosens. Bioelectron.*, 2019, **130**, 147–165.
149 A. M. Jimenez Jimenez, M. A. M. Rodrigo, V. Milosavljevic, S. Krizkova, P. Kopel, Z. Heger and V. Adam, *Sens. Actuators, B*, 2017, **240**, 503–510.
150 C. S. Kim, D. Ingato, P. Wilder-Smith, Z. Chen and Y. J. Kwon, *Nano Convergence*, 2018, **5**, 3.
151 Y. Liu, S. H. Wu, X. Y. Du and J. J. Sun, *Sens. Actuators, B*, 2021, **338**, 129854.
152 T. Pinheiro, A. C. Marques, P. Carvalho, R. Martins and E. Fortunato, *ACS Appl. Mater. Interfaces*, 2021, **13**, 3576–3590.
153 D. Chakraborty, A. Mukherjee and K. R. Ethiraj, *Anal. Methods*, 2022, **14**, 3614–3622.
154 A. Pal, S. K. Dubey and S. Goel, *Comput. Electron. Agric.*, 2022, **195**, 106856.
155 A. Pal, M. B. Kulkarni, H. Gupta, R. N. Ponnalagu, S. Kumar Dubey and S. Goel, *Sens. Actuators, A*, 2021, **330**, 112896.
156 D. Li, Y. Dong, B. Li, Y. Wu, K. Wang and S. Zhang, *Analyst*, 2015, **140**, 7672–7677.